



**STATENS GEOTEKNISKA INSTITUT**

SWEDISH GEOTECHNICAL INSTITUTE

**No. 50**

**SÄRTRYCK OCH PRELIMINÄRA RAPPORTER**

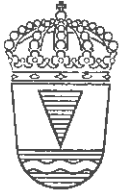
**REPRINTS AND PRELIMINARY REPORTS**

Supplement to the "Proceedings" and "Meddelanden" of the Institute

**Damping of Stress Waves in Piles during  
Driving. Results from Field Tests**

**Gunnar Fjelkner & Bengt Broms**

STOCKHOLM 1972



**STATENS GEOTEKNISKA INSTITUT**

SWEDISH GEOTECHNICAL INSTITUTE

No. **50**

**SÄRTRYCK OCH PRELIMINÄRA RAPPORTER**

**REPRINTS AND PRELIMINARY REPORTS**

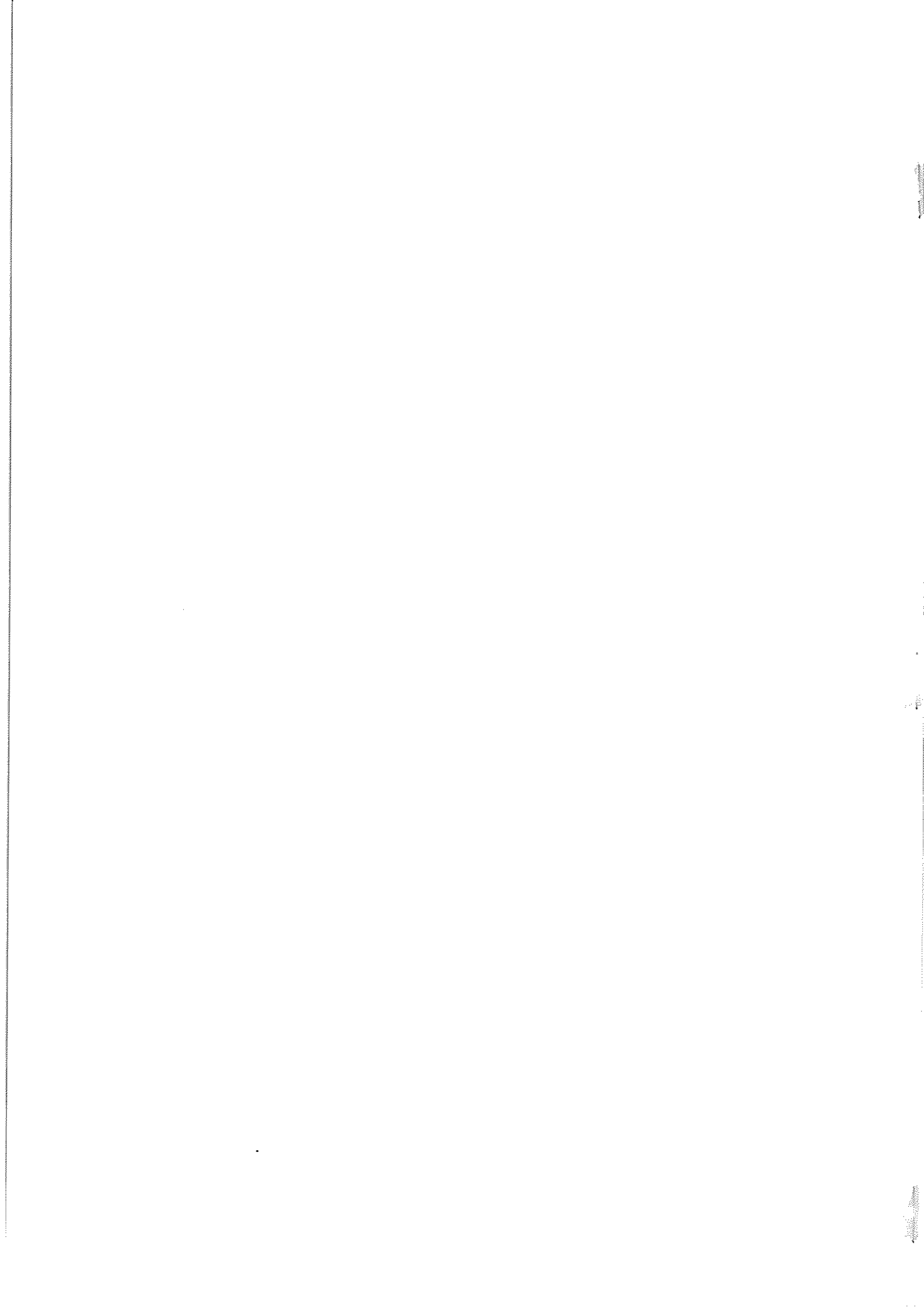
Supplement to the "Proceedings" and "Meddelanden" of the Institute

**Damping of Stress Waves in Piles during  
Driving. Results from Field Tests**

**Gunnar Fjelkner & Bengt Broms**

Also included in IVA, Pålkommissionen, Meddelande No. 19

**STOCKHOLM 1972**



## PREFACE

The pile driving formula included in the Swedish Building Code takes into account the damping caused by friction or adhesion along the pile shaft. Little is, however, known about the effect of the roughness of the pile surface on the damping in different soils. To improve the knowledge in this respect the investigation presented in this report has been performed.

The work is part of the program within the Pile Research Commission of the Swedish Academy of Engineering Sciences (IVA). It has mainly been carried out at the Swedish Geotechnical Institute with financial support of the Swedish Board for Building Research (Grant No. C 497) and of the Swedish Commission for Pile Research.

Stockholm, December 1972

SWEDISH GEOTECHNICAL INSTITUTE

## CONTENTS

	Page
Summary	3
1. INTRODUCTION	4
2. THEORY	5
3. TEST EQUIPMENT	8
Test piles	8
Instrumentation	8
Calibration	10
Pile driving rig	12
Cap block and cushion	15
4. TEST SITES	16
5. TEST PROCEDURE	19
Driving of test piles	19
Driving diagrams	19
Stress wave measurement	20
6. TEST RESULTS	27
Amplitude damping	27
Computer-calculated damping	34
Pulling tests	39
7. CONCLUSIONS	41
ACKNOWLEDGEMENTS	42
REFERENCES	42

## DAMPING OF STRESS WAVES IN PILES DURING DRIVING

by Gunnar W. Fjellner and Bengt B. Broms

### SUMMARY

The decrease of the amplitude (the damping) of the stress wave as it travels down a pile during driving, has been investigated. The damping has been measured by strain gauges attached to the inside surface of four steel pipe piles with 89 mm (3.5 in) outside diameter. One of the test piles was tested unsupported in an open shaft in order to investigate the damping in the pile material and in the welded joints. Two test piles were driven through sand; one of these had a rough surface while the surface of the second pile was smooth. The fourth test pile which had a smooth surface was driven through soft clay.

Measurements show that the damping in the steel material and in the welded joints is small and negligible in comparison with the damping caused by friction or adhesion along the pile surface. The damping in the piles with a smooth surface was found to be about the same for sand as for clay. The amplitude decreased by about 1 percent/meter length of pile while the damping for the pile with the rough surface which was driven through sand was 2 to 3 percent/meter. The same amount of damping was also observed for the fourth test pile with a smooth surface surrounded by clay, when the pile was redriven a few months after the initial driving.

The observed damping was found to be proportional to the particle velocity in the pile. On the basis of this observation an equation has been derived which relates the damping with the pile material, the pile diameter, the cross-sectional area and the pile length.

## 1. INTRODUCTION

Driven precast piles are commonly used in Sweden. According to a survey by the Swedish Commission on Pile Research 65 percent of all piles installed in Sweden are of this type. Precast concrete piles are generally driven by a 3 to 4 tons drop hammer. The height of fall is normally 30 to 60 cm (1 to 2 ft).

A stress wave is generated when the ram strikes the head of a pile during the driving. This stress wave travels down the pile with the velocity of sound which for a steel pile is 5 100 meter/sec (16 700 ft/sec). The maximum amplitude of the stress wave decreases as the wave travels down the pile due to friction or adhesion of the soil along the pile shaft. Also the shape of the stress wave is changed. Due to the decrease the force and the displacement at the pile point can be small if the pile is long and a light ram is used during the driving. This is often a problem for the very long end-bearing piles which are commonly used in the southwestern parts of Sweden.

Few direct measurements of the damping during the driving have been reported in the literature. Glanville et al. (1938) have measured the damping in full-scale reinforced concrete piles. Test data indicate that the damping in such piles can be very high. In a series of tests carried out by the Commission on Pile Research of the Swedish Academy of Engineering Sciences (1964) with reinforced concrete piles which were driven into a deep layer of soft clay at Gubbero, located in Gothenburg in the southwestern part of Sweden, the damping with respect to the peak stress (the amplitude) was 0.6 percent/meter length of pile.

Smith (1960) has calculated the stress distribution during driving of a pile from the assumption that the friction resistance along the pile shaft is proportional to the particle velocity. This assumption has been substantiated by this investigation. However, Gibson and Coyle (1968) have found from laboratory tests that the dynamic friction resistance in their case is not quite proportional to the particle velocity.

The bearing capacity of driven piles is often calculated from the driving resistance. Sovinč (1969) has reported for a steel pile which was driven into sand and gravel that the dynamic skin friction resistance along the pile surface during the driving was about 80 percent of the static resistance determined afterwards from

a pile load test. These results thus indicate that the skin friction resistance during driving can deviate considerably from the static resistance also for cohesionless soils.

In this article is described the results from driving tests on four steel pipe piles. One pile was tested unsupported in an open shaft, two piles were driven through a deposit of sand and one pile through a layer of clay.

## 2. THEORY

There are several different definitions of the term damping as illustrated in Fig. 1. The ratio  $(A_1 - A_2)/A_1$  represent the damping between two adjacent levels with respect to the maximum amplitude, while the ratio  $(B_1 - B_2)/B_1$  is the damping at a given time  $t$  after the arrival of the stress wave. The ratio  $(E_1 - E_2)/E_1$  represents the energy damping between two adjacent levels.

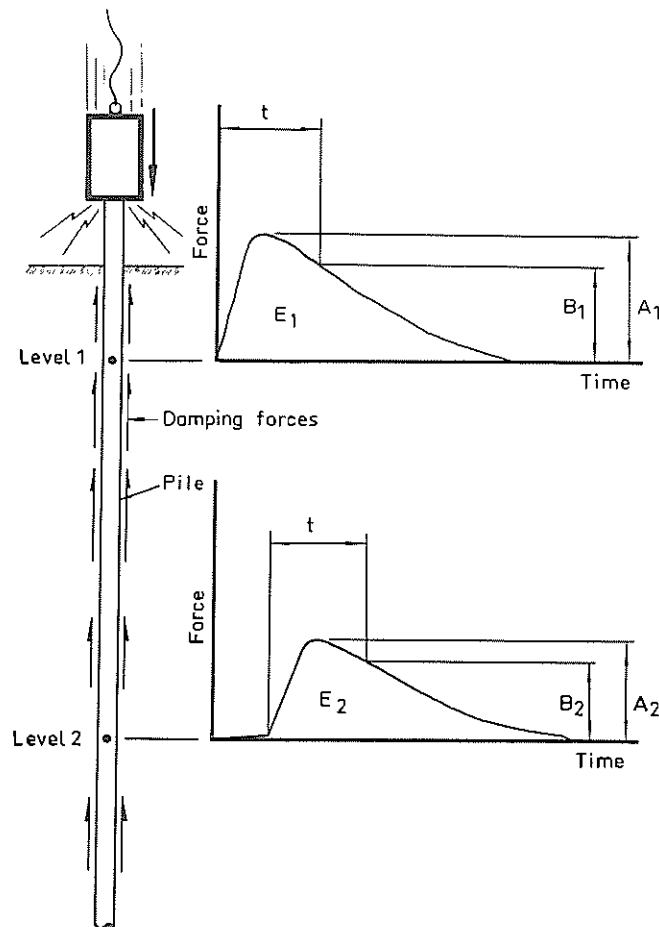


Fig. 1. Different ways to define damping. The figure shows the stress wave in a pile on level 1 and 2.



Damping is defined in this report as the ratio  $(A_1 - A_2)/A_1$ . This definition of damping can, for example, be used in connection with pile driving formulas of the stress wave type. The equation proposed by Fjellner (1971) is an example of such a formula which takes into account the amplitude damping. It is also possible to consider damping in pile driving formulas of the energy type since the energy is proportional to the integral  $\int P^2 dt$ , where  $P$  is the axial dynamic force in the pile. If the damping at each interval of the stress wave is proportional to the force  $P$ , the energy damping will be proportional to  $(A_1^2 - A_2^2)/A_1^2$ .

The decrease of the amplitude between two adjacent levels is dependent on the properties of the soil around the pile (shear strength, sensitivity, angle of internal friction, etc.), the roughness of the pile surface, the lateral earth pressure acting on the pile shaft, the shaft area and the particle velocity in the pile material.

The effect of soil properties, surface roughness, and lateral earth pressure has in this investigation been taken into account through a coefficient  $C_1$ . It has been assumed in the following that the damping is directly proportional to the surface area of the pile as expressed by the proportionality coefficient  $C_2$  and to the particle velocity as expressed by the proportionality coefficient  $C_3$ .

The relationship between the particle velocity  $v_p(z)$  at a distance  $z$  from the pile head, the propagation velocity of the stress wave ( $c_p$ ), the modulus of elasticity of the pile material ( $E_p$ ), the cross-sectional area of the pile ( $A_p$ ) and the axial force  $P_i(z)$  at the distance  $z$  can be expressed by the following equation

$$v_p(z) = \frac{c_p}{E_p A_p} P_i(z) \quad (1)$$

However, the axial force in the pile  $P_i(z)$  is decreased by  $dP_i(z)$  as the wave travels the distance from  $(z)$  to  $(z + dz)$  as shown in Fig. 2.

With the assumptions made above the change  $dP_i(z)$  of the axial force can be calculated from

$$dP_i(z) = - C_1 C_2 C_3 O_p v_p(z) dz \quad (2)$$

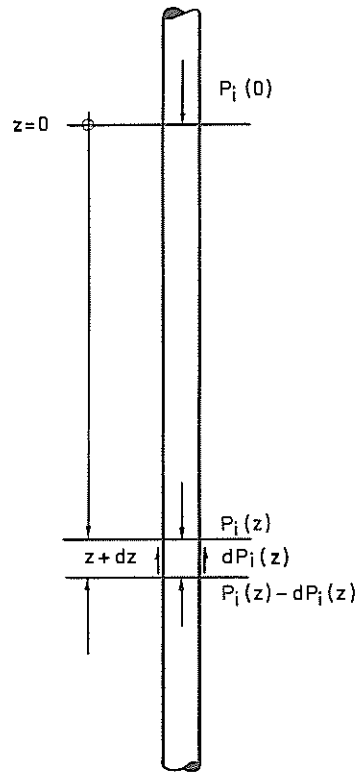


Fig. 2. Amplitudes at adjacent levels in a pile.

where  $O_p$  is the circumference of the pile. The product  $(C_1 C_2 C_3)$  has in this investigation been substituted by the coefficient  $C_d$  (force x time/length<sup>3</sup>, e.g. kNs/m<sup>3</sup>) which in this report is called the damping coefficient. Then from Eqs. (1) and (2)

$$\frac{dP_i(z)}{dz} + \frac{C_d O_p c P_i(z)}{E_p A_p} = 0 \quad (3)$$

One solution to this differential equation is

$$P_i(z) = P_i(0) \cdot e^{-\frac{C_d O_p c z}{E_p A_p}} \quad (4)$$

where  $P_i(0)$  is the force at level 0, e.g. at the pile head. This equation indicates that the maximum amplitude of the stress wave will decrease exponentially with depth.

### 3. TEST EQUIPMENT

Test piles. The damping as the stress wave travels down a pile has been investigated in four steel test piles of about half the normal size (Table I). The test piles had an outside and an inside diameter of 89 mm (3.5 in) and 79 mm (3.1 in), respectively. The cross-sectional area was  $13 \text{ cm}^2$  (2.0 sq in) and the circumference 0.28 meter (11 in). Each test pile was composed of a number of 1.5 m (5 ft) long segments which were welded together (Fig. 3). Each test pile was provided with a solid steel point with the dimensions shown in Fig. 4.

TABLE I. Test piles A, C, F and R

Pile No	Pile surface	Soil	Test site
Pile A	Smooth	None	
Pile C	Smooth	Clay	Ultuna
Pile F	Smooth	Sand	Fittja
Pile R	Rough	Sand	Fittja

Three of the test piles had an untreated smooth surface which was somewhat oily and without any rust. Sand was glued to the surface of the fourth test pile to create a rough surface. The pile segments of this pile were first brushed with epoxy resin which had been diluted with acetone. The segments were then rolled in G 12 sand, which is a beach sand of marine origin with rounded particles and an average grain size ( $D_{50}$ ) of 0.24 mm. The G 12 sand has been used in numerous investigations at the Danish Geotechnical Institute and at the Swedish Geotechnical Institute. This sand has been described in detail e.g. by Orrje (1968).

Instrumentation. The stresses in the test piles which developed during the driving were measured by strain gauges glued to the inside surface of the test piles to protect the gauges from damage during the driving. The gauges were placed at some distance from the joints to avoid damage of the gauges during the welding. The cables which were attached to the strain gauges inside the tube were protected during the welding by a short brass tube which was lowered down to the welding level. This tube was covered by asbestos.



Fig. 3. The investigations were made on steel piles with 89 mm outside and 79 mm inside diameter. The pile segments before welding are shown above.

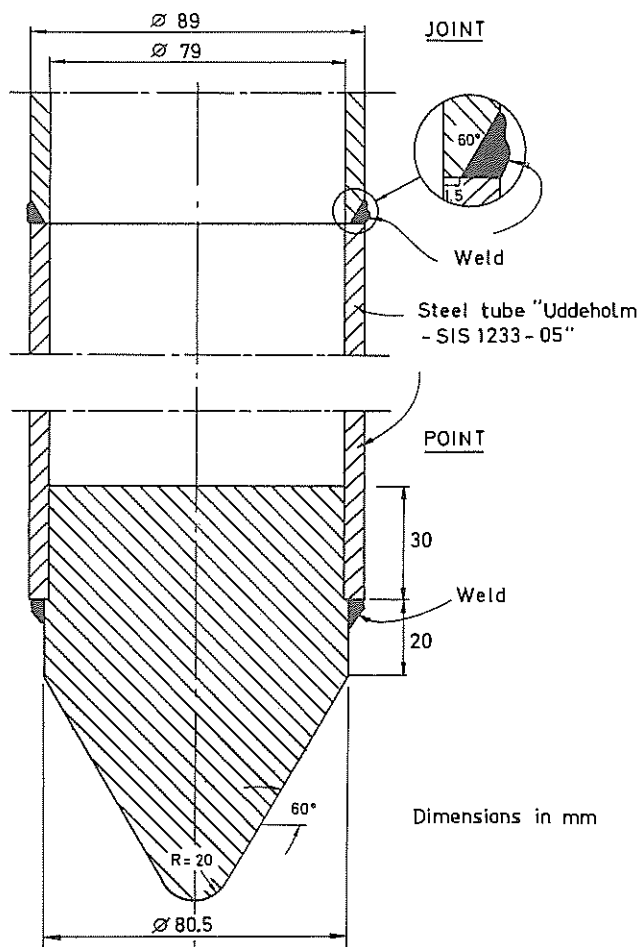


Fig. 4. Pile joint and pile point.

The inside diameter of the pile segments was however too small to allow the placement of the strain gauges by hand. Each gauge and the corresponding cable were therefore first attached to a strip of plastic tape. The tape and the gauge were then placed upside down in the 0.65 meter long pile segment after glue had been brushed on the gauge. The segments were thoroughly cleaned in advance. The gauge was pressed down by a roller which was inserted into the tube as shown in Fig. 5.

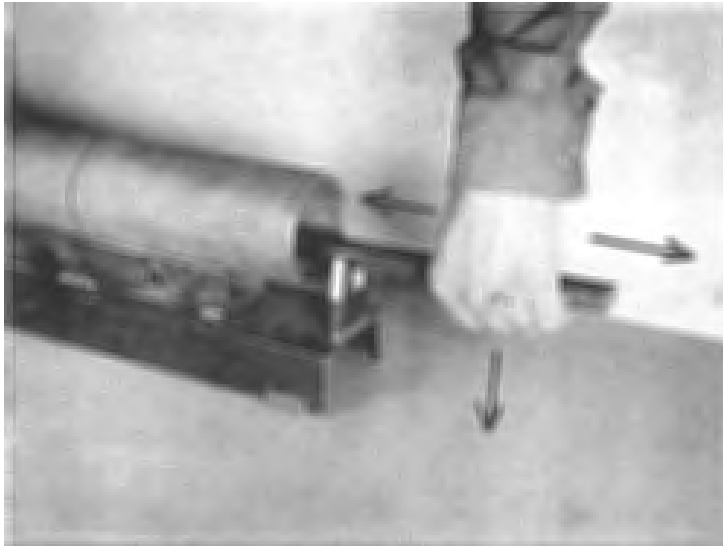


Fig. 5. During gluing, strain gauges were pressed down with a roller.

Four strain gauges were placed at each measuring level. All gauges were provided with separate cables, so that each gauge could be read separately in case a gauge would fail. Two diametrically placed strain gauges were used as active gauges as shown in Fig. 6. The cables were shielded by aluminium foil which was wound around the cables as can be seen in Fig. 7. The measured stress waves were displayed on an oscilloscope screen and photographed by a polaroid camera. Two oscilloscopes, Tektronix 564 with amplifier 3A3, were used during the tests.

Calibration. The strain gauges were calibrated by loading each segment axially in increments up to 50 metric tons (500 kN). The applied axial force was measured by a load cell. All strain gauges were recalibrated after the piles had been pulled.

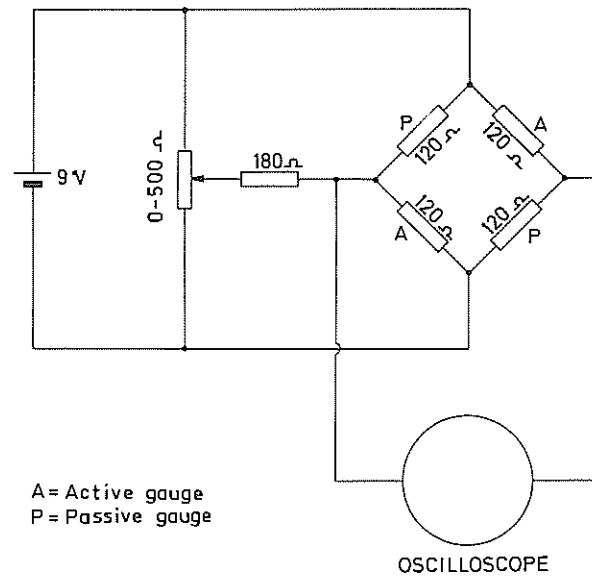


Fig. 6. Strain gauge circuit. A potentiometer was used to balance the gauge bridge.



Fig. 7. Arrangement for the driving tests. The cables from the strain gauges were shielded with aluminium foil.

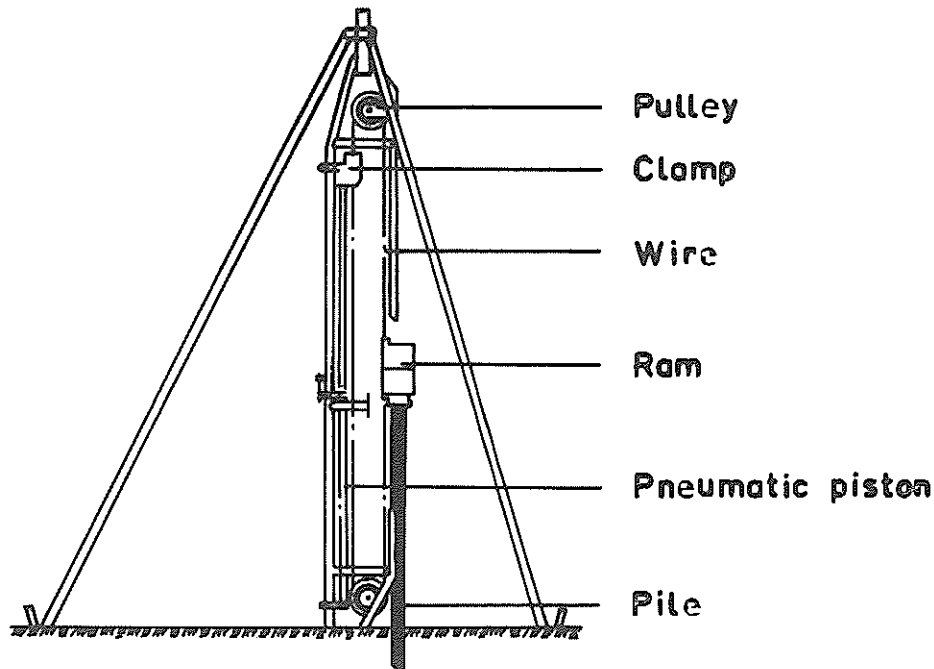


Fig. 8. Pile driving rig.

The strain gauge readings should theoretically not be affected by a bending moment since the active gauges were placed diametrically opposite in the tube. The calibrations indicated, however, that an eccentricity of the applied load had a slight effect on the readings. The calibrations were therefore made with care to keep the eccentricity of the applied load as small as possible.

The striking velocity of the ram was measured by a velocity meter as described by Sundström (1970). The measured velocity values were used to calculate the friction losses in the pile driving rig which was used for the driving tests in sand and clay. The measured average striking velocity corresponded to a calculated equivalent height of free fall which was 0.015, 0.02, and 0.02 meter less than the nominal heights of 0.37, 0.46, and 0.56 meter, respectively. Thus about 4 percent of the total energy was lost during the fall due to friction and inertia effects.

Pile driving rig. Three of the test piles were driven by the pile driving rig shown schematically in Fig. 8. The 200 kg (440 lbs) ram was lifted by a steel wire which passed over two pulleys. The wire was gripped by a ball-clamp attached to a pneumatic piston. The pile driver was driven by compressed air

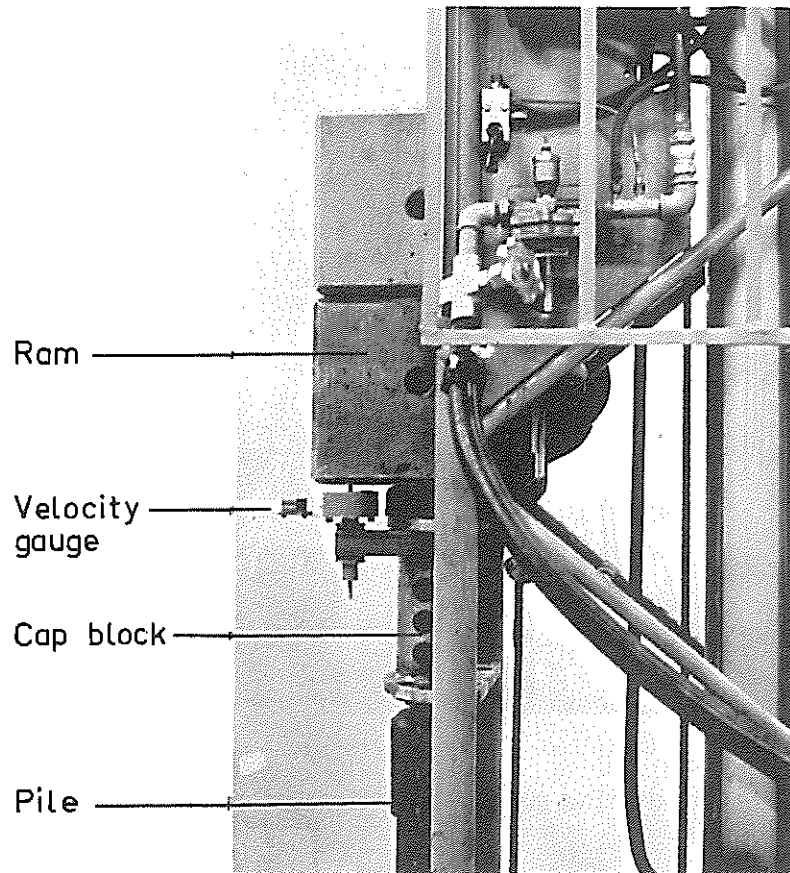


Fig. 9. Ram, capblock and pile. The striking velocity of the ram is measured by the gauge attached to the cap-block.

from an air compressor with a maximum capacity of about  $2 \text{ m}^3/\text{minute}$ . The driving was regulated automatically (30 blows/minute) or manually. The height of fall could be varied continuously between 0 and 1.5 meter. The ram, the cap block of the pile driver and the head of the test pile are shown in Fig. 9.

The pile driving rig described above could not be used for the tests which were carried out in an open shaft due to lack of head room. A special driving rig, shown in Fig. 10, was therefore constructed, where the 200 kg ram was lifted by a winch. The ram was released by cutting the wire holding the ram.



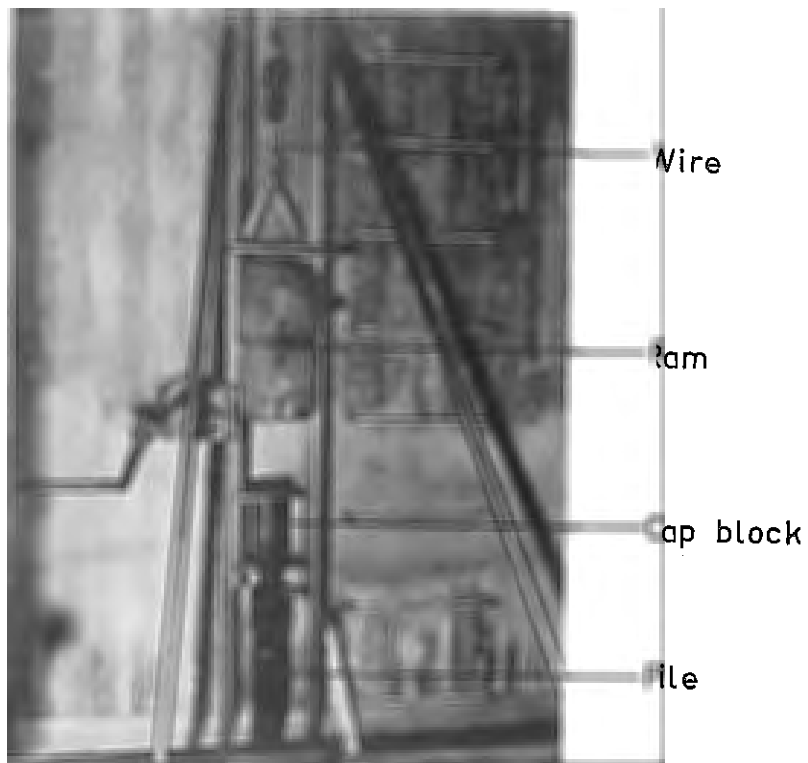


Fig. 10. Pile driving rig for investigation on the unsupported pile.

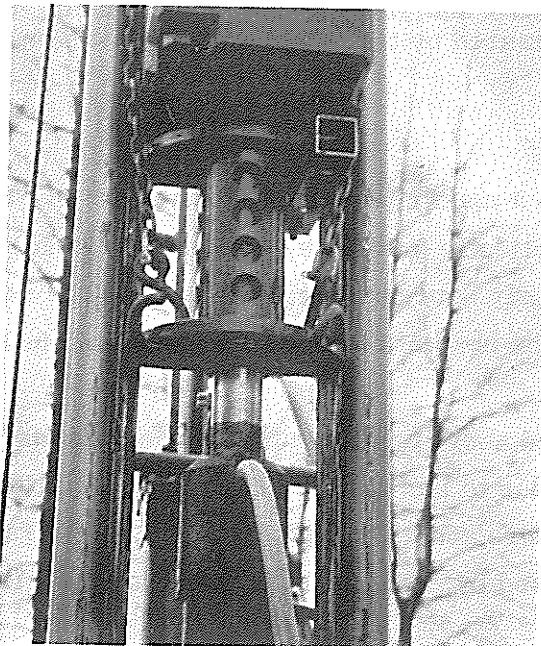
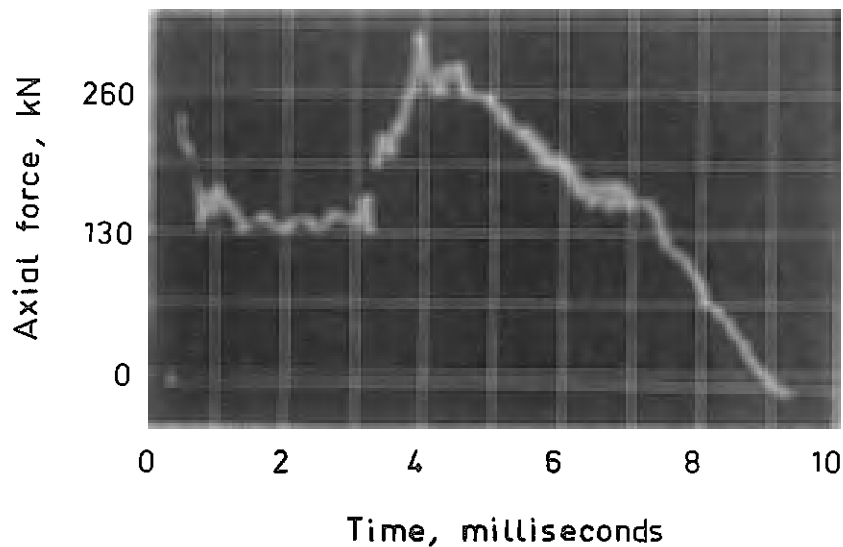


Fig. 11. Front view of ram, capblock and pile. The ram and the upper part of the capblock is lifted to show the lower part (the piston) of the capblock.

Cap block and cushion. The cap block consists of two parts, a piston and a cylinder (Fig. 11). The shape of the stress wave could be changed by changing the thickness and the properties of the 50 mm diameter cushion which was placed between the piston and the cylinder. Different cushion materials were investigated in order to reproduce the shape and the intensity of the stress waves in full size piles as closely as possible. First, wooden cushions and relatively stiff cushions of leather and of other similar materials were investigated. Thereafter, successively softer rubber cushions were tested.

A rubber cushion with a total thickness of 20 mm (0.8 in) was finally chosen for the main experiments. The quality of the rubber was about the same as that of an inner tube for a car. This type of cushion was found to withstand several thousand blows without a change of the properties of the stress wave. The shape of the stress wave when a 200 kg ram struck a 7 meter long steel pile with 89 mm outside and 79 mm inside diameter without a cushion in the capblock is shown in Fig. 12. The corresponding stress wave when a 20 mm thick rubber cushion was used can be seen in Fig. 13. This stress wave is much smoother than that shown in Fig. 12.



Height of fall: 1.0 m

Ram : 200 kg

Pile length : 7 m

Fig. 12. Stress wave record from a 7 m long testpile. No cushion in the capblock. The wave which is reflected at the pile point arrives about 3 milliseconds after the initial wave.

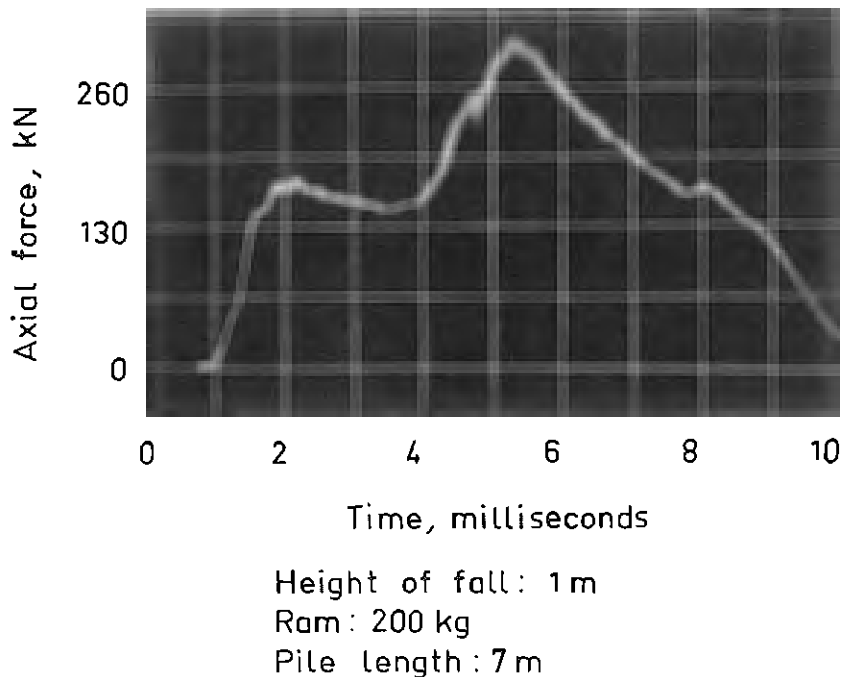


Fig. 13. Stress wave record for the same conditions as in fig. 12 except for a 20 mm rubber cushion which was placed inside the capblock. The high peaks observed in fig. 12 have disappeared.

#### 4. TEST SITES

One of the test piles was investigated in a 23 meter high open shaft at Teknikum at the University of Uppsala in Sweden. These tests were carried out in order to investigate the damping caused by the pile material and by the welded joints. The pile was supported laterally at three levels to prevent buckling of the pile. The pile point rested on a steel plate placed on a heavy concrete block.

A test site at Ultuna, located 60 km north of Stockholm, was chosen for the tests in clay. This test site has been described in detail by Kallstenius (1963). A typical soil profile is shown in Fig. 14. It can be seen that the clay at this test site is relatively uniform with an undrained shear strength which varies between 20 and 30 kN/m<sup>2</sup> (2.8 and 4.2 psi). The water content of the clay decreases from 100 percent at a depth of 5 meter to about 60 percent at a depth of 15 to 20 meter below the ground surface.

Sampling with Swedish standard piston sampler

Weight sounding

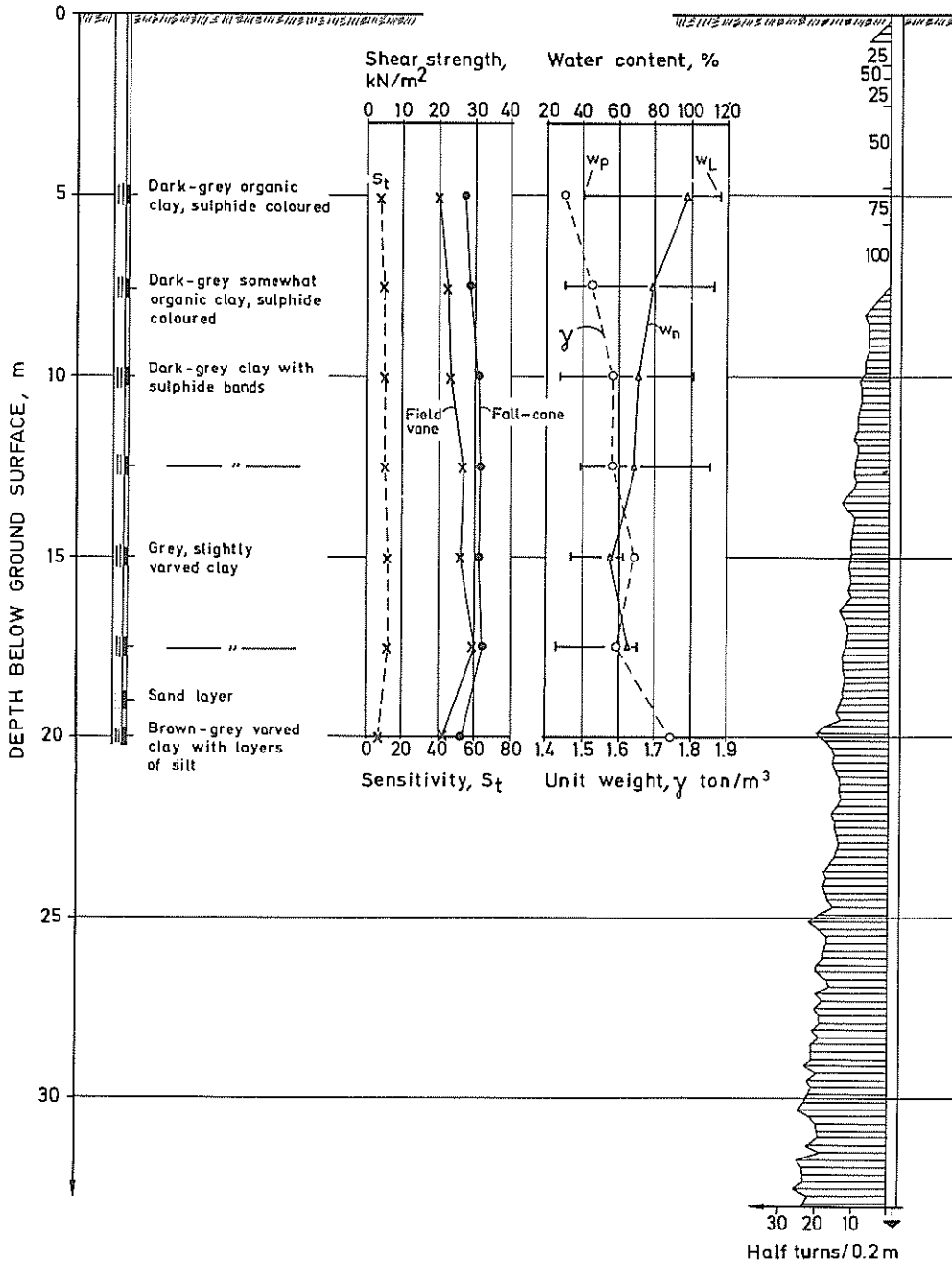


Fig. 14. Soil investigations at Ultuna (Kallstenius 1963).

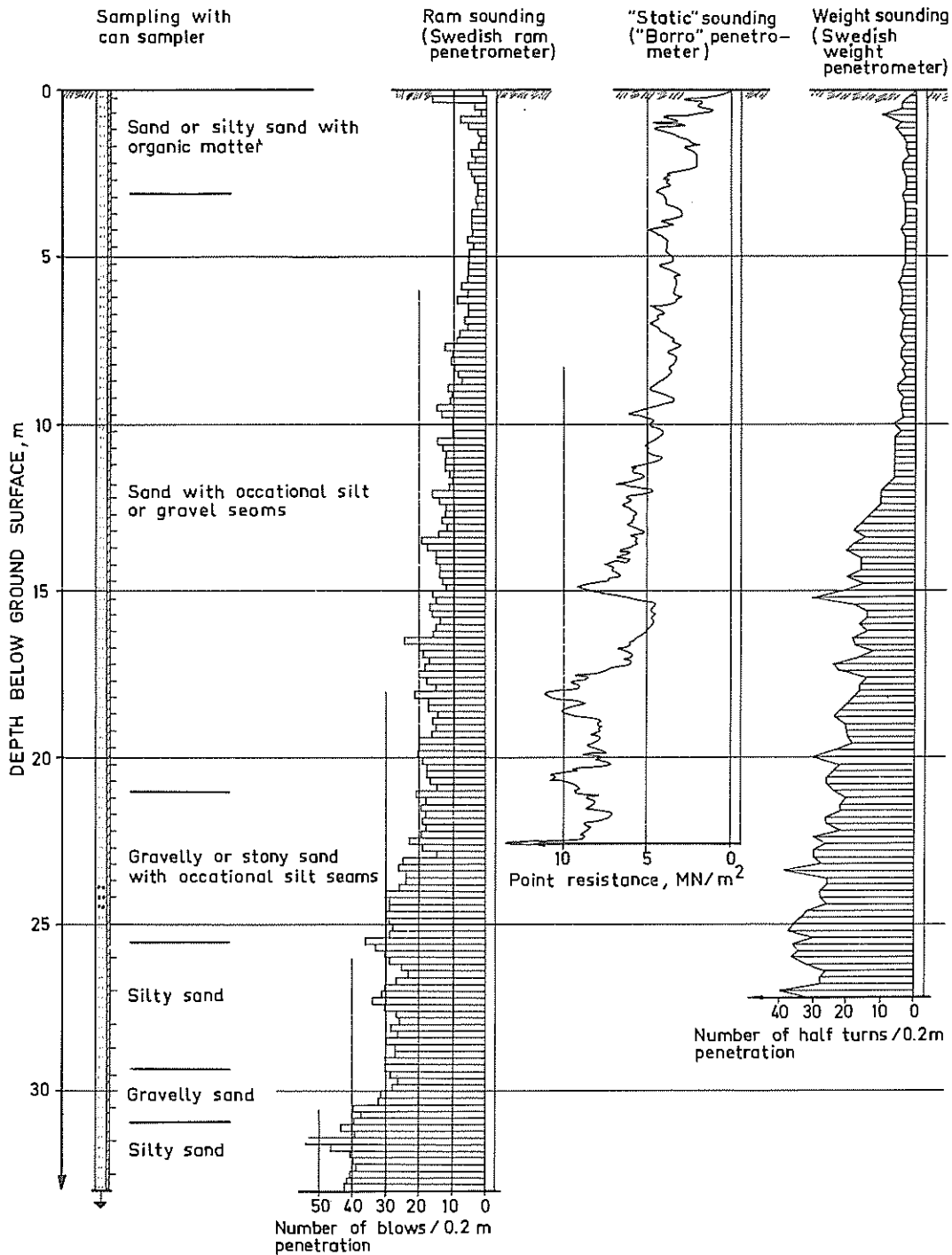


Fig. 15. Soil investigations at Fittja. The ram sounding was made with a free falling height of 0.5 m. The static penetration tests was made with the Borro penetrometer where the force at the point, with  $10 \text{ cm}^2$  cross sectional area, is measured with strain gauges.

The test in sand was carried out at Fittja, located 15 km south-west of Stockholm. The soil conditions at this test site are uniform as indicated by borings and soundings (Fig. 15). The penetration resistance of the soil as measured by ram or weight soundings was found to increase with depth. The increase was, however, not as pronounced with the "Borro" static penetrometer which also was used. The shape and the diameter of the "Borro" penetrometer point is the same as that of the Dutch cone penetrometer. (The cross-sectional area is  $10 \text{ cm}^2$  and the apex angle 60 degrees.) The force at the penetrometer point for the "Borro" penetrometer is measured with strain gauges. Thus friction along the penetrometer rod will not affect the test results in contrast to the ram or the Swedish weight penetrometer. The penetration resistance of the "Borro" penetrometer is thus expected to be about the same as for the Dutch cone penetrometer.

## 5. TEST PROCEDURE

Driving of test piles. The steel piles were driven by a 200 kg ram using the pile driving rig shown in Fig. 8. The cushion in the capblock was replaced before each test. The height of fall of the ram was 0.5 m (1.6 ft) when the penetration resistance was low. The height was increased to 0.8 (2.7 ft) or 1.2 (4.0 ft) meter when the resistance increased. The number of blows required to drive the pile was recorded.

Driving diagrams. The driving resistance of pile C, which was driven in clay, is shown in Fig. 17 as a function of depth. It can be seen that 2 700 blows were required to drive the pile to a total depth of 31.6 meter (104 ft). The height of fall of the 200 kg ram was 0.5 meter. It is interesting to note how the penetration resistance increased with time. When the pile was redriven 50 days after the initial driving the penetration resistance had increased seven times.

The driving diagram of Pile F, which was driven in sand to a total depth of 28.0 meter (92 ft), is shown in Fig. 18. The height of fall was 0.5 meter until the pile had been driven to a depth of 24 meter (79 ft) below the ground surface. Below this depth the height of fall was increased to 0.8 meter. About 5 000 blows were required to reach the final depth.

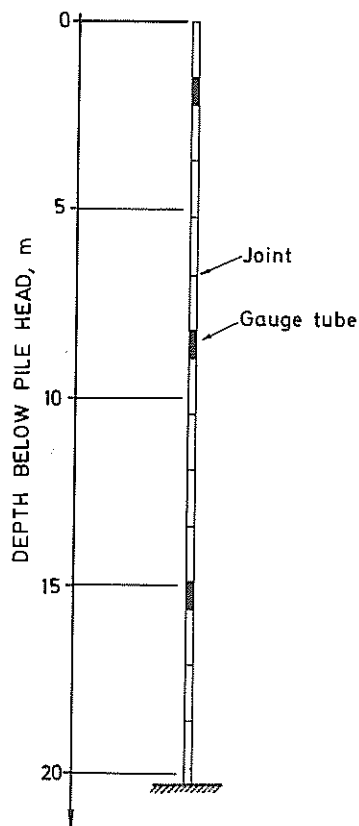


Fig. 16. Location of strain gauges in Pile A which was standing free in an open shaft.

The measured driving resistance of Pile R, which had a rough surface, is shown in Fig. 19. The pile was driven through sand down to a total depth of 13.5 meter (44 ft) below the ground surface. About 1 600 blows were required. The height of fall was 0.8 meter until the pile had reached a depth of 12.5 meter (41 ft). Below this depth the height was increased to 1.2 meter. At 13.5 meter the penetration of the pile for each blow was almost zero. About the same total number of blows was required to drive Pile F and Pile R down to a depth of 10 meter (33 ft) even though the height of fall and therefore the delivered energy was 60 percent higher for Pile R than for Pile F. This difference in behaviour is attributed to the difference in surface roughness between the two piles.

Stress wave measurements. The intensity and the shape of the stress waves which developed during the driving were measured at nine different occasions. One series of measurements was made on Pile A, four on Pile C, three on Pile F, and one on Pile R. The relative position of the piles during the nine test series are shown in Figs. 16 through 19.

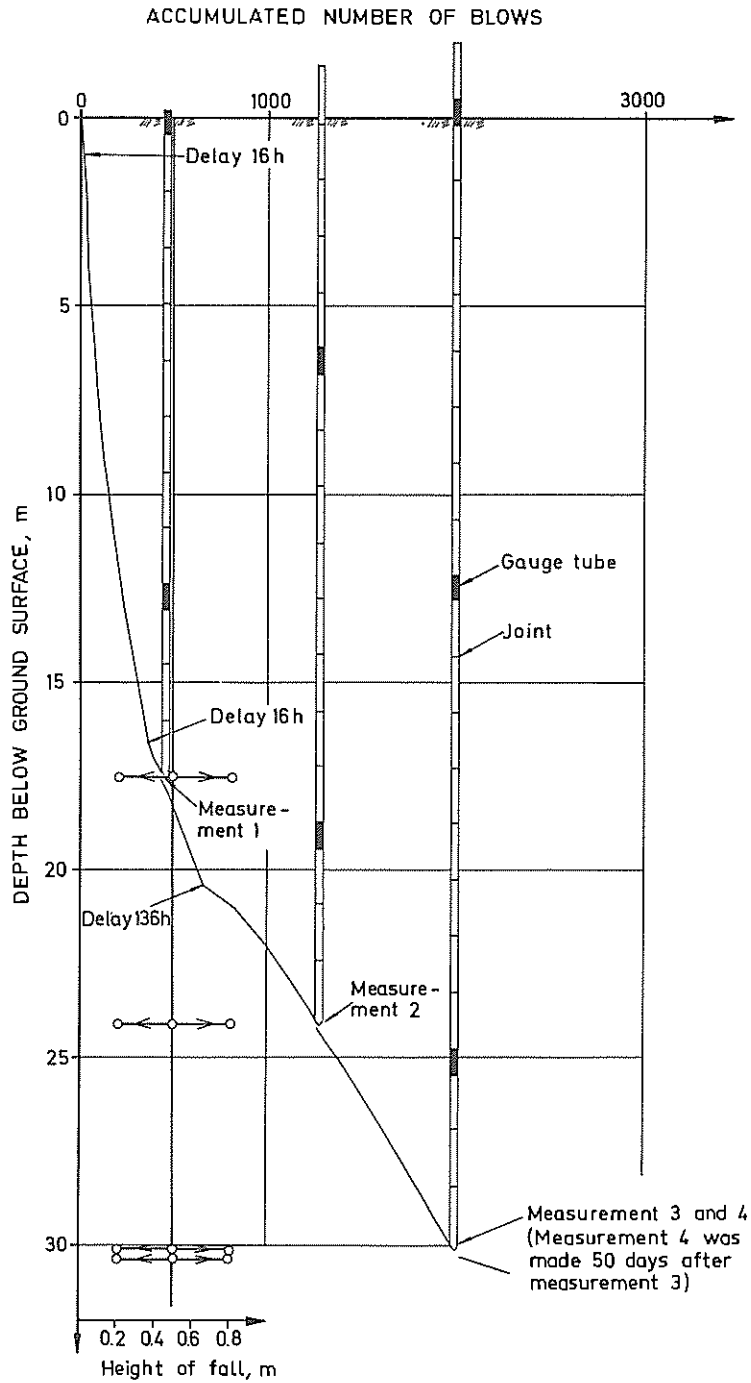


Fig. 17. Driving diagram and location of strain gauges at measurements on Pile C which had a smooth steel surface and was driven in clay.



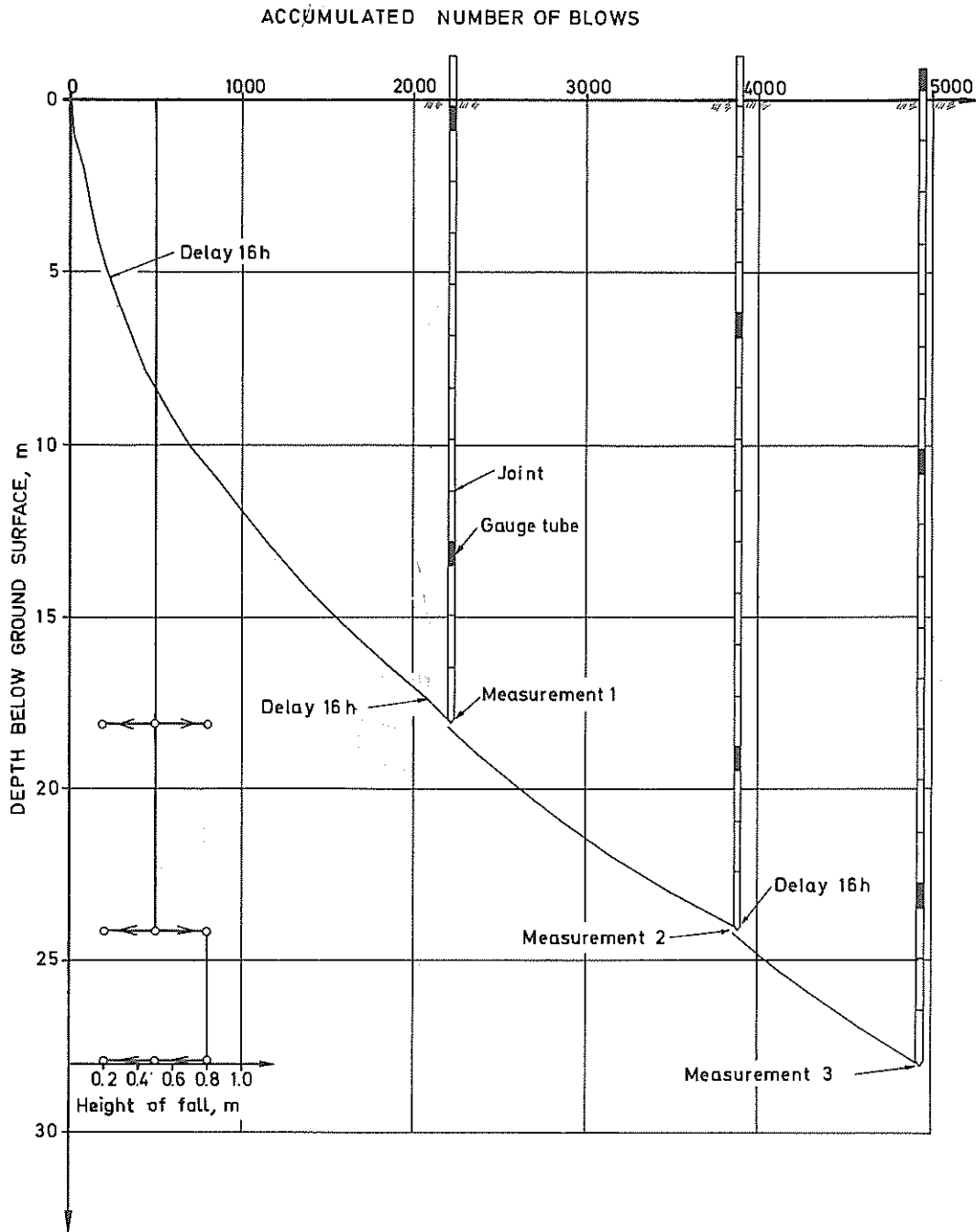


Fig. 18. Driving diagram and location of strain gauges at measurements on Pile F which had a smooth steel surface and was driven in sand.

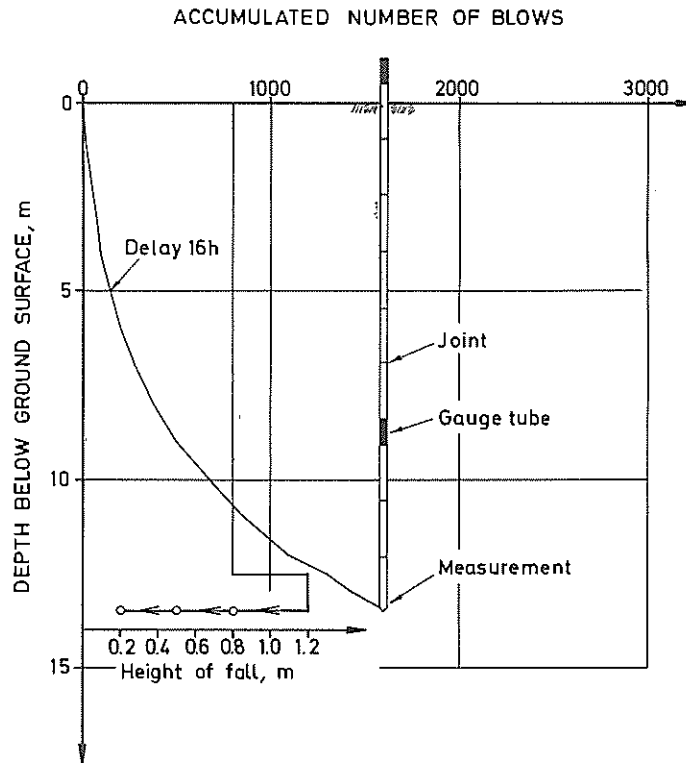
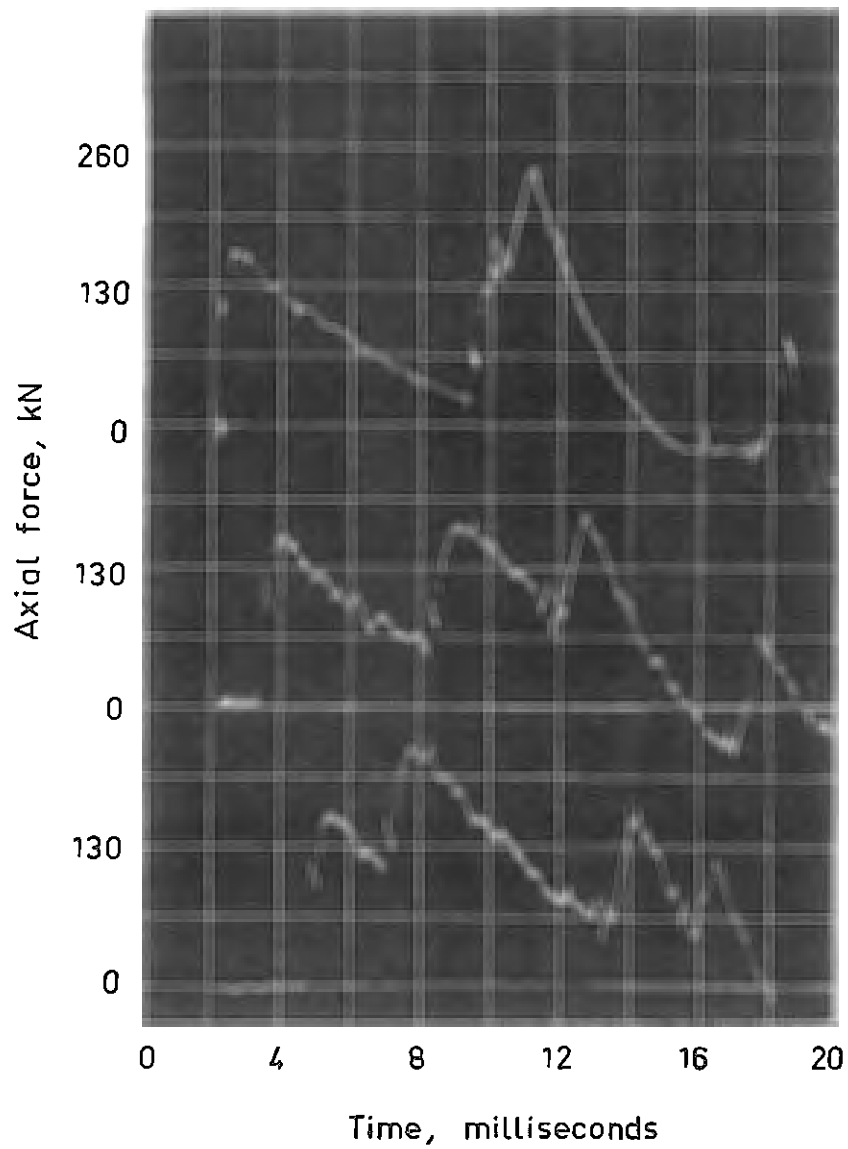


Fig. 19. Driving diagram and location of strain gauges at the measurement on Pile R which had a rough surface and was driven in sand.

The heights of fall for each test series were 0.2, 0.5 and 0.8 meter. Several separate measurements were made for each height. Typical stress wave records are shown in Figs. 20 to 23 when the height of fall was 0.8 meter. The individual records have been placed in order with respect to the different measuring levels. Since the oscilloscope sweeps were started at the same time it is possible to follow the propagation and the resulting changes of the stress wave as it travels down the pile and is reflected at the pile point.

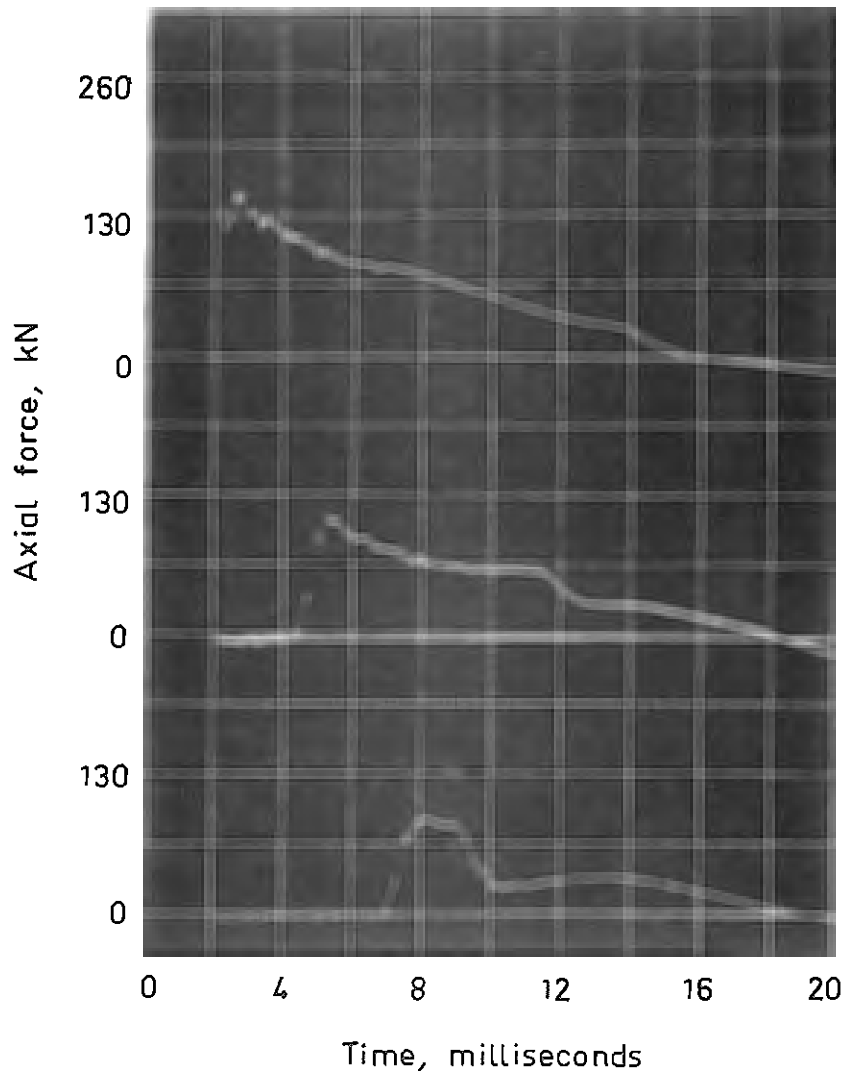
The stress wave records shown in Figs. 20 to 23 at the four different measuring levels indicate that the maximum amplitude of the initial wave is reached about 1 millisecond after the wave front arrived to a particular location. Almost the same amplitude was obtained at the upper measuring level, indicating that the height of fall and the properties of the cushion have almost been the same at the four different test series (Figs. 20, 21, 22 and 23).

For Pile A the maximum amplitude was almost the same at the three measuring levels. For the other three piles the maximum amplitude decreased with increasing depth.



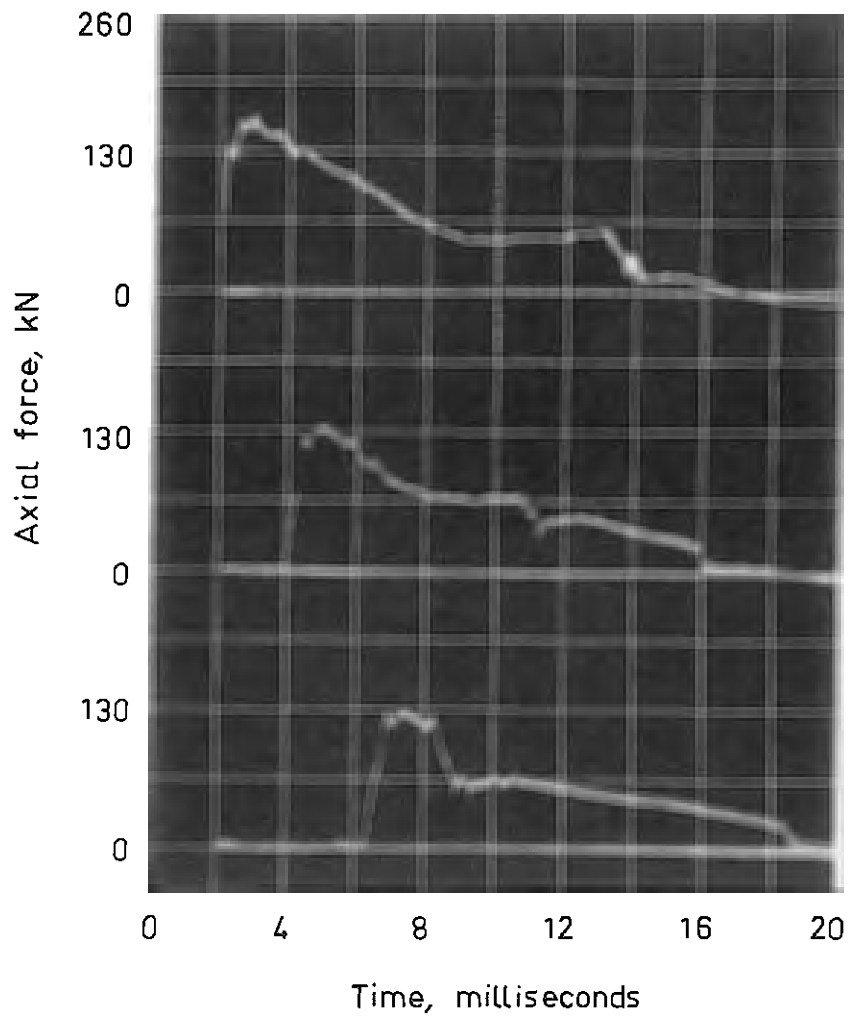
Height of fall: 0.8 m  
Ram: 200 kg

Fig. 20. Stress wave records from Pile A which was standing in an open shaft. The three measuring levels are shown in fig. 16.



Height of fall: 0.8 m  
Ram : 200 kg  
Pile surface : Smooth  
Soil : Clay

Fig. 21. Stress wave records from Pile C. The three measuring levels are shown in fig. 17 (measurement 4).



Height of fall : 0.8 m  
Ram : 200 kg  
Pile surface : Smooth  
Soil : Sand

Fig. 22. Stress wave records from Pile F. The three measuring levels are shown in fig. 18 (measurement 3).

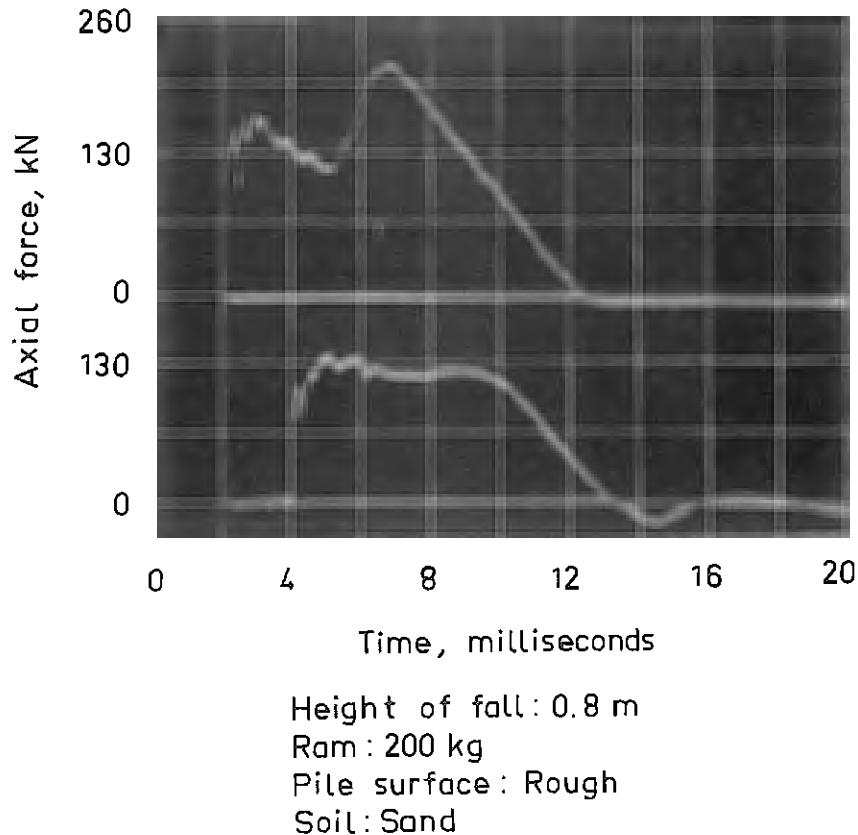


Fig. 23. Stress wave records from Pile R. The two measuring levels are shown in fig. 19.

## 6. TEST RESULTS

Amplitude damping. In Figs. 24 to 32 are shown the change of the maximum amplitude of the initial stress wave as it travelled down the pile. The amplitudes were measured when the heights of fall were 0.2, 0.5 and 0.8 meter. No significant damping was found for Pile A, which was standing free in an open shaft (Fig. 24). These results indicate that the damping in the steel material or in the welded joints was negligible. For Pile C, which was driven through a layer of clay (Figs. 25, 26, 27) the damping was about constant and independent of depth. The damping increased, however, with time. When the pile was redriven 50 days after the initial driving the damping was about twice that when the pile first was driven (Fig. 28). The amplitude damping for Pile F, which was driven through sand, was about the same as that for Pile C, which was driven through clay. The surface of

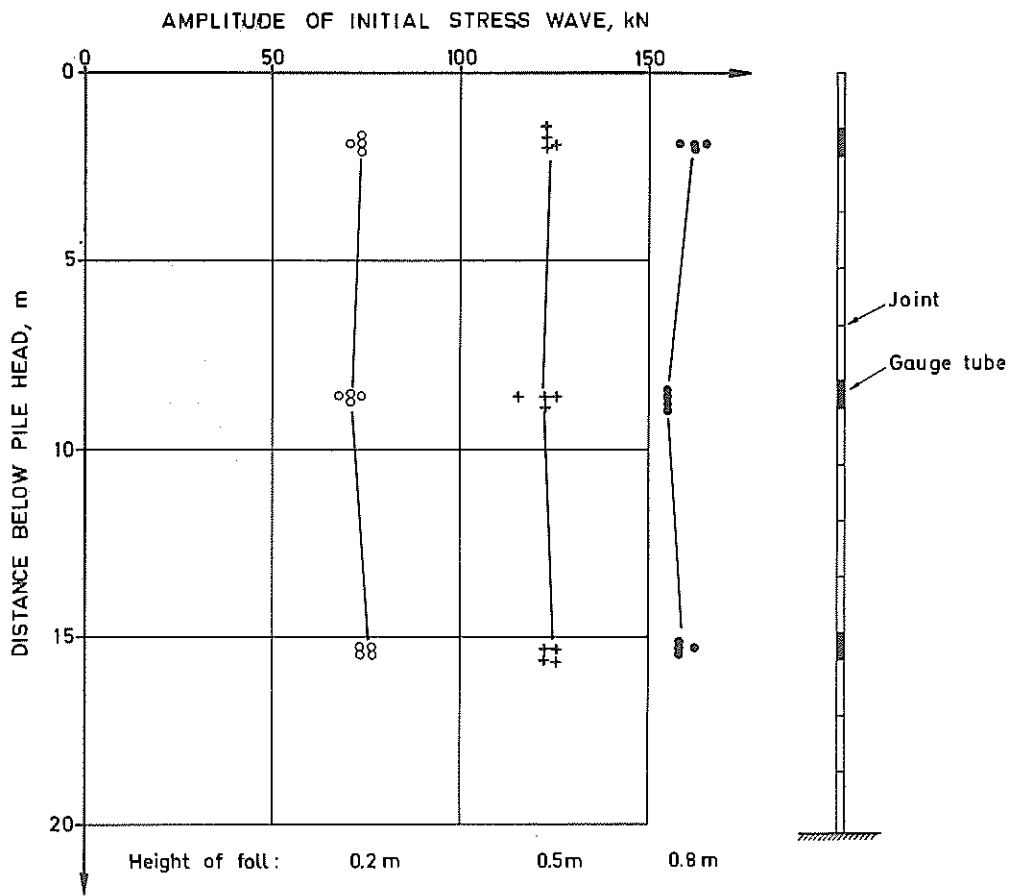


Fig. 24. Amplitudes of the initial stress waves at different heights of fall in Pile A.

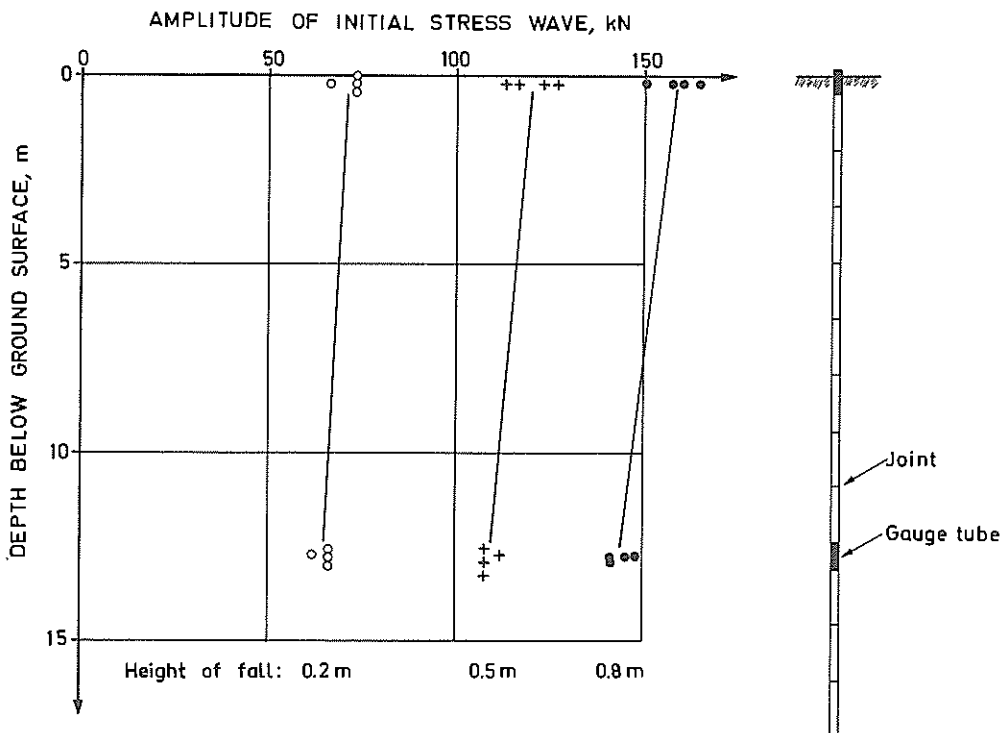


Fig. 25. Amplitudes of the initial stress waves at different heights of fall in Pile C (measurement 1).

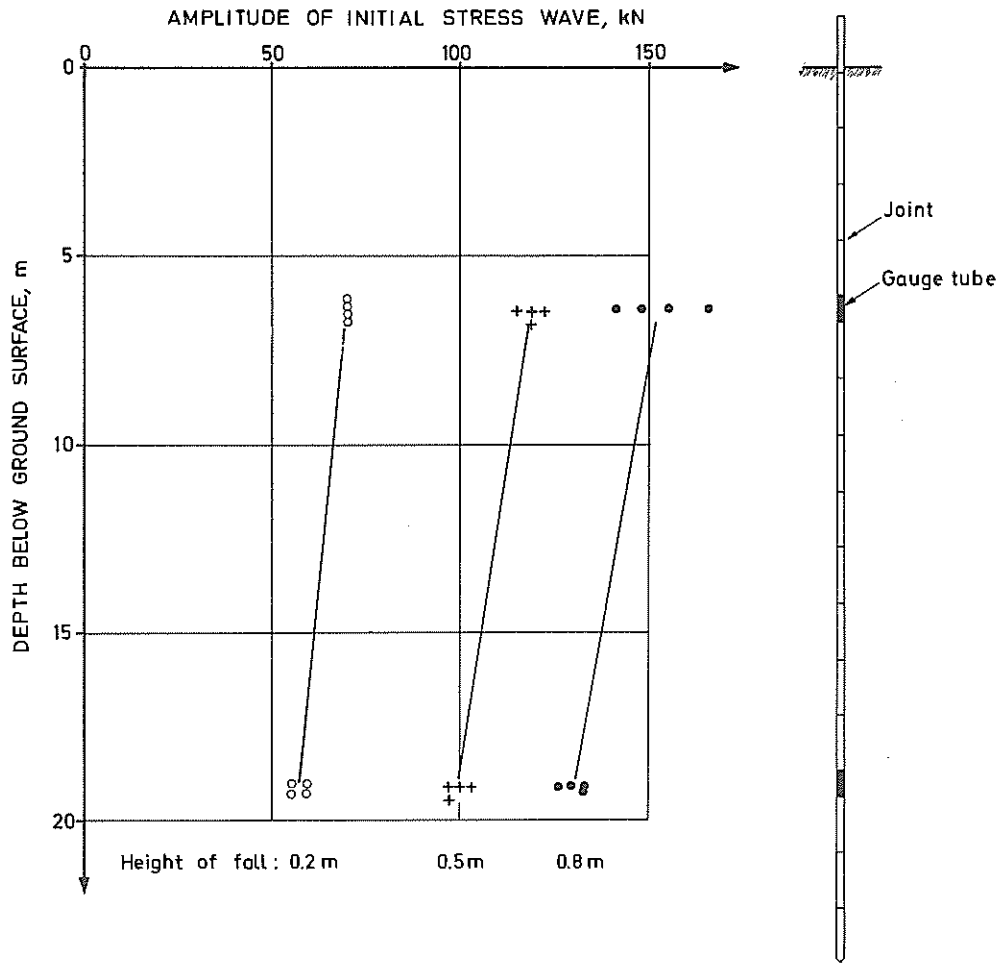


Fig. 26. Amplitudes of the initial stress waves at different heights of fall in Pile C (measurement 2).



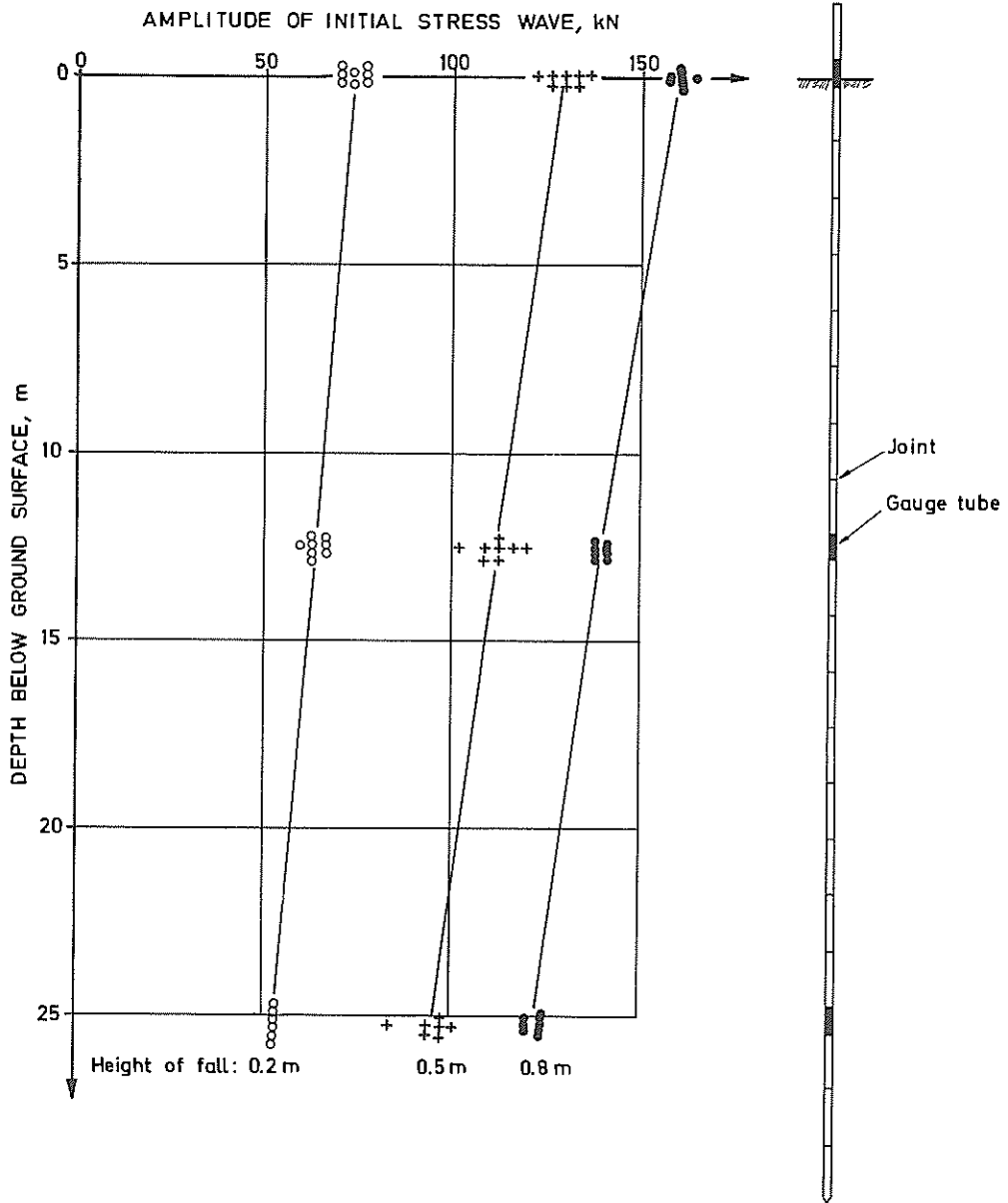


Fig. 27. Amplitudes of the initial stress waves at different heights of fall in Pile C (measurement 3).

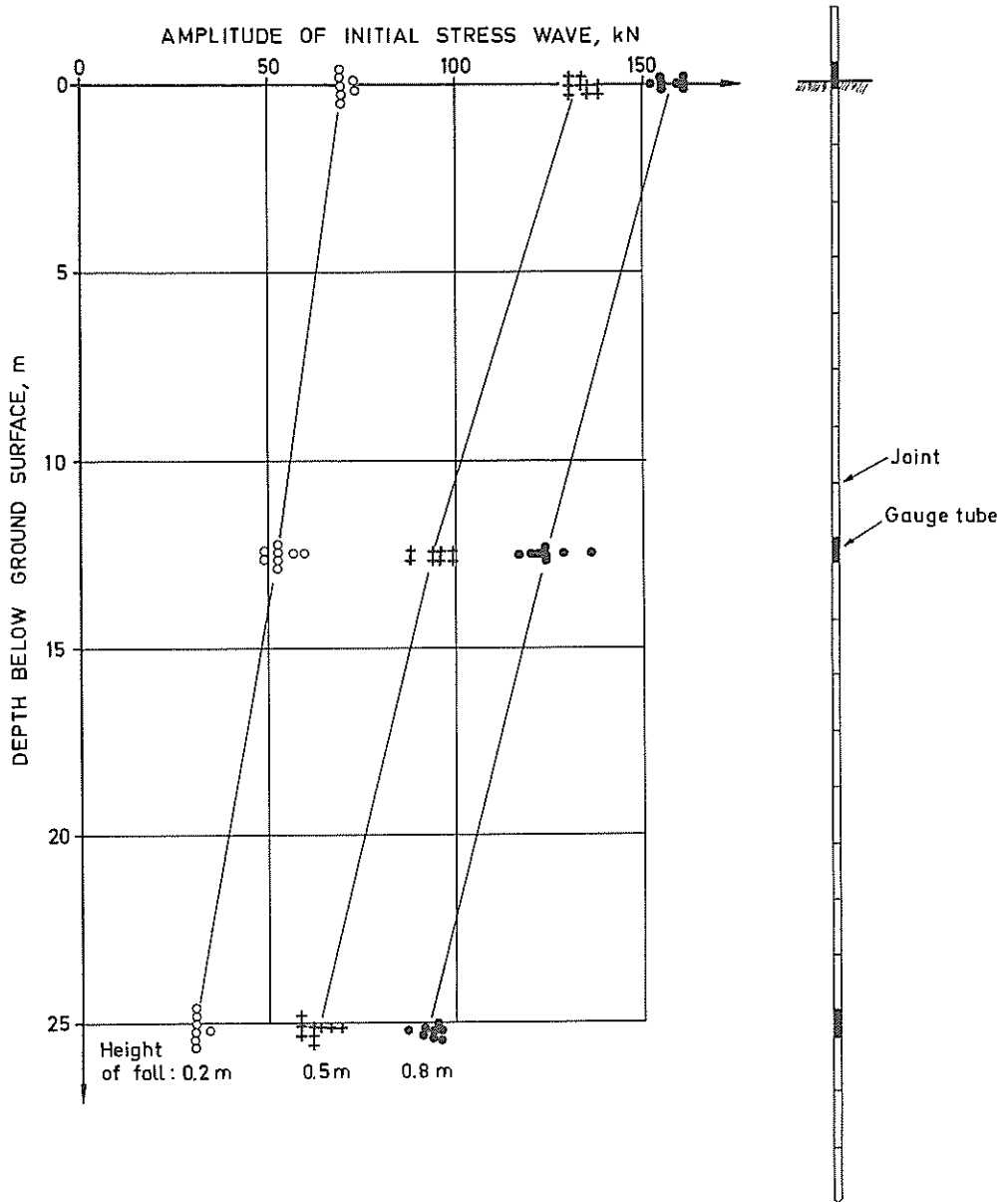


Fig. 28. Amplitudes of the initial stress waves at different heights of fall in Pile C (measurement 4).

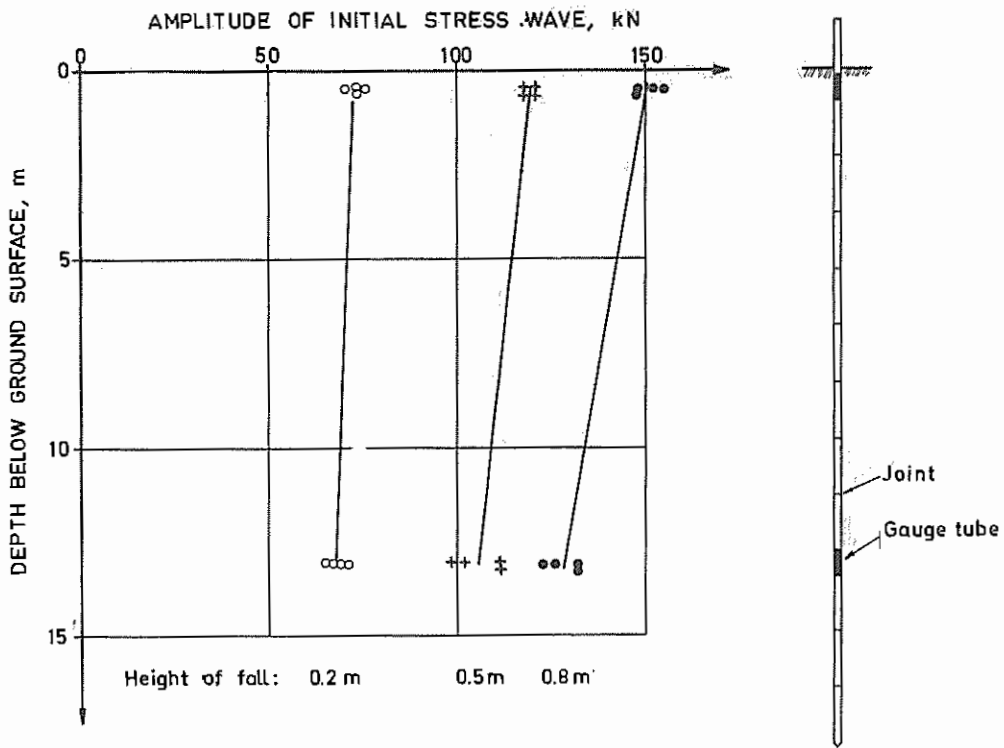


Fig. 29. Amplitudes of the initial stress waves at different heights of fall in Pile F (measurement 1).

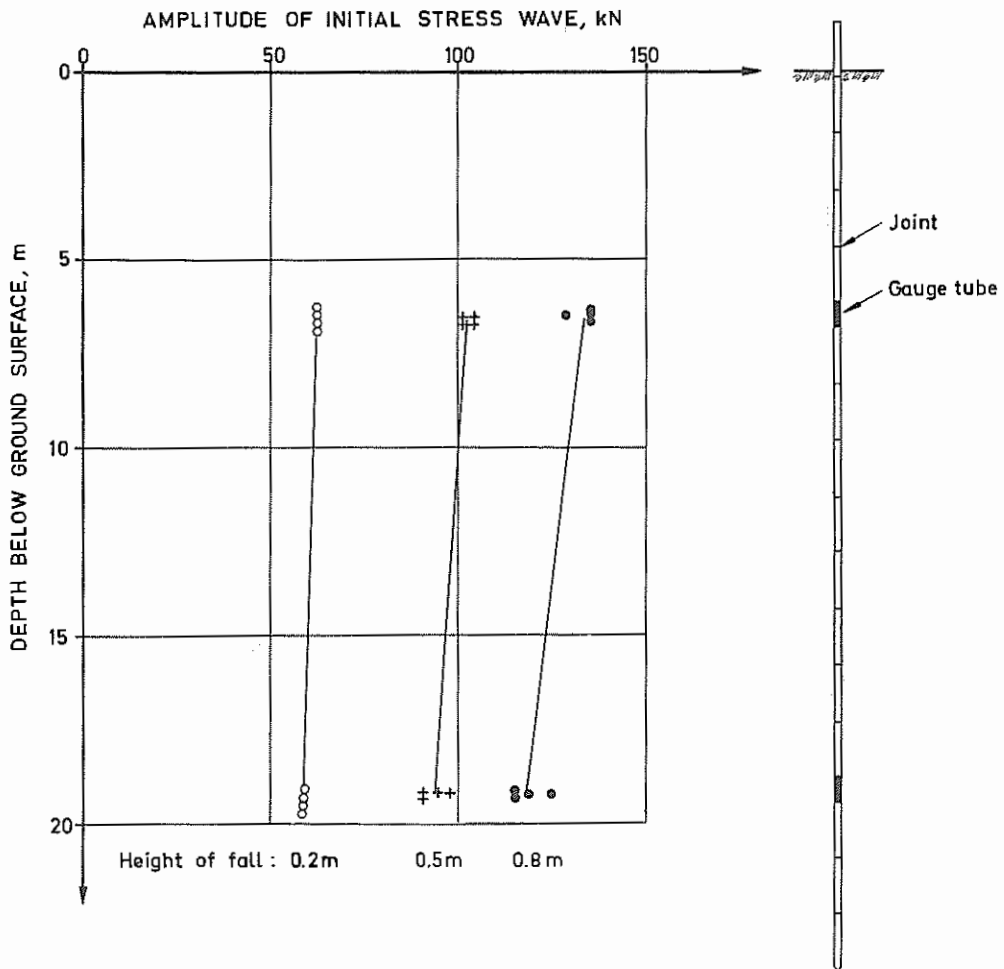


Fig. 30. Amplitudes of the initial stress waves at different heights of fall in Pile F (measurement 2).

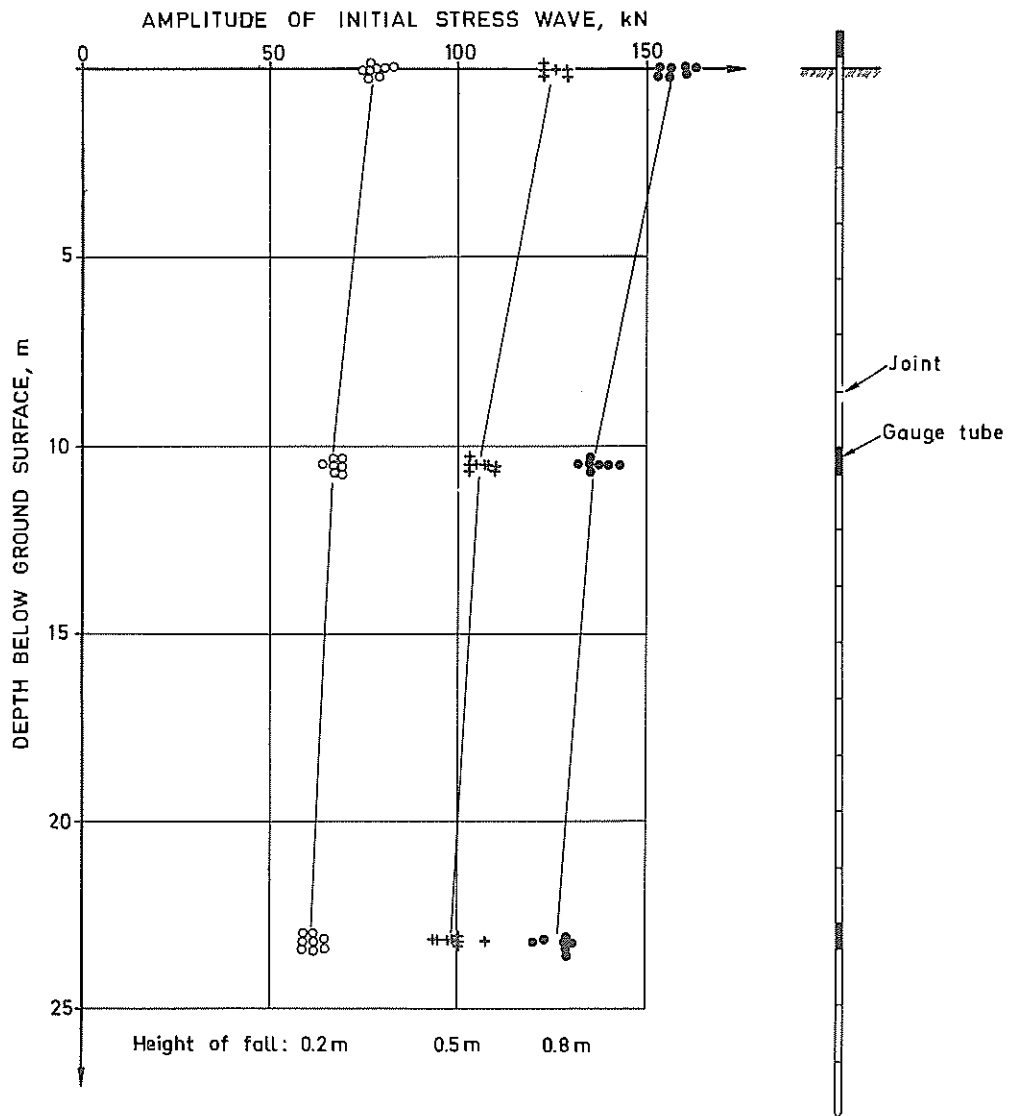


Fig. 31. Amplitudes of the initial stress waves at different heights of fall in Pile F (measurement 3).

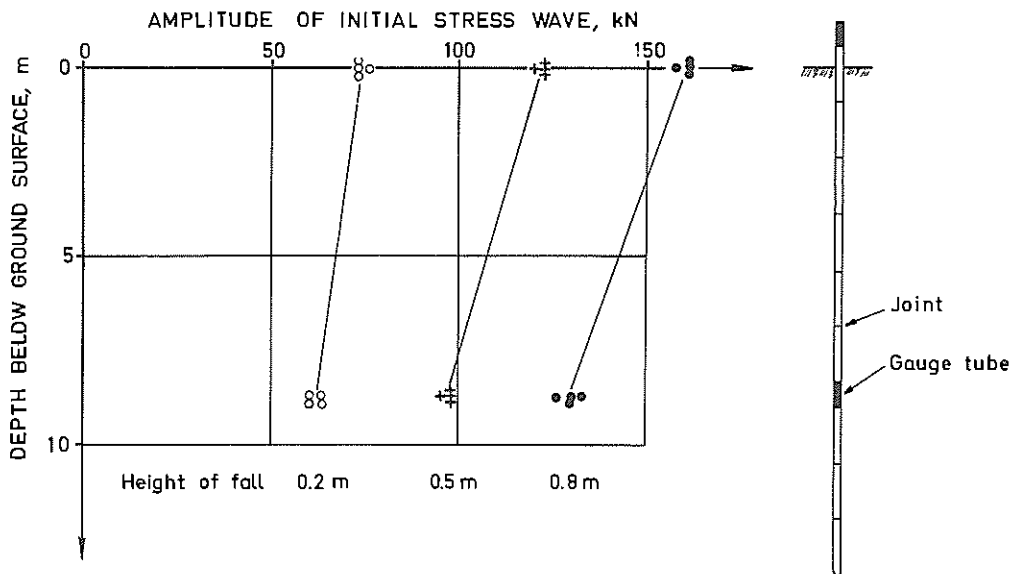


Fig. 32. Amplitudes of the initial stress waves at different heights of fall in Pile R.

the two piles was smooth. The relative damping for Pile F decreased however somewhat with depth. Pile R, which had a rough surface and was driven through sand, had an amplitude damping which was about twice that of Pile F.

The test results from the four test piles are summarized in Table II. The damping coefficient  $C_d$  in this table has been evaluated from Eq. (4). The relationship between damping and particle velocity can be evaluated by comparing the calculated values of the damping coefficient  $C_d$  for different heights of fall when all other factors were kept constant. It can be seen that the damping coefficient was approximately independent of the height of fall. According to Table II the ratio  $C_d/C_{d, \text{average}}$  was equal to 1.04, 0.95 and 1.01 when the height of fall was 0.2, 0.5 and 0.8 meter, respectively. It was therefore concluded that the amplitude damping for the investigated piles was approximately proportional to the particle velocity as was assumed in the derivation of the damping equation.

The average value of  $C_d$  was  $2.16 \text{ kNs/m}^3$  ( $20.0 \text{ lb sec/ft}^3$ ) for Pile C during the initial driving, and  $5.34 \text{ kNs/m}^3$  ( $49.5 \text{ lb sec/ft}^3$ ) when the pile was redriven 50 days later. For Pile F the average value of  $C_d$  was  $1.83 \text{ kNs/m}^3$  ( $17.0 \text{ lb sec/ft}^3$ ) while for Pile R the average value was  $4.48 \text{ kNs/m}^3$  ( $41.8 \text{ lb sec/ft}^3$ ).

Computer-calculated damping. The shape and intensity of the stress wave at the pile head can be calculated from the strain gauge readings using the computer program which has been described by Vilander (1969). Different distributions of the friction forces has been assumed until the calculated intensity and the shape of the stress wave at a particular location agreed with the measured ones.

The stepped curves shown in Figs. 34 through 37 are results from computer calculations. The best fits are given using the assumed skin friction distribution indicated in Fig. 33. The dashed curves are measured values which correspond to the recorded stress waves shown in Figs. 20 through 23.

The measured and calculated relationships for Pile A which was standing free in an open shaft, are shown in Fig. 34. The agreement is satisfactory except for the first part of the curve. This part is, however, influenced to a large extent by the properties of the cushion in the cap block.

TABLE II. Evaluation of the damping coefficient  $C_d$ 

Pile	Soil	Measure- ment	Damping measured between depths m	Height of fall m	Damping coefficient		
					$C_d$ kNs/m <sup>3</sup>	$C_{d, aver}$ kNs/m <sup>3</sup>	$\frac{C_d}{C_{d, aver}}$
C	clay - smooth steel surface	1	0.2	0.2	1.35		0.94
			and	0.5	1.47		1.03
			12.7	0.8	1.47	1.43	1.03
		2	6.4	0.2	3.09		1.15
			and	0.5	2.63		0.98
			19.1	0.8	2.34	2.69	0.87
		3	0.0	0.2	2.11		0.99
			and	0.5	2.22		1.04
			12.5	0.8	2.10	2.14	0.98
			12.5	0.2	2.84		1.18
			and	0.5	2.40		1.00
			25.2	0.8	1.95	2.40	0.81
4	0.0	0.2	4.50		1.01		
	and	0.5	5.30		1.19		
	12.5	0.8	3.59	4.46	0.80		
	12.5	0.2	8.17		1.31		
	and	0.5	6.02		0.97		
	25.2	0.8	4.47	6.22	0.72		
F	sand - smooth steel surface	1	0.5	0.2	1.08		0.60
			and	0.5	1.88		1.05
			13.1	0.8	2.40	1.79	1.34
		2	6.5	0.2	0.75		0.49
			and	0.5	1.39		0.91
			19.2	0.8	2.43	1.52	1.60
		3	0.0	0.2	2.77		1.00
			and	0.5	3.00		1.08
			10.5	0.8	2.55	2.77	0.92
			10.5	0.2	1.42		1.15
			and	0.5	1.19		0.97
			23.2	0.8	1.09	1.23	0.89
R	sand - rough steel surface	0.0	0.2	3.88		0.87	
		and	0.5	4.92		1.10	
		8.7	0.8	4.64	4.48	1.04	

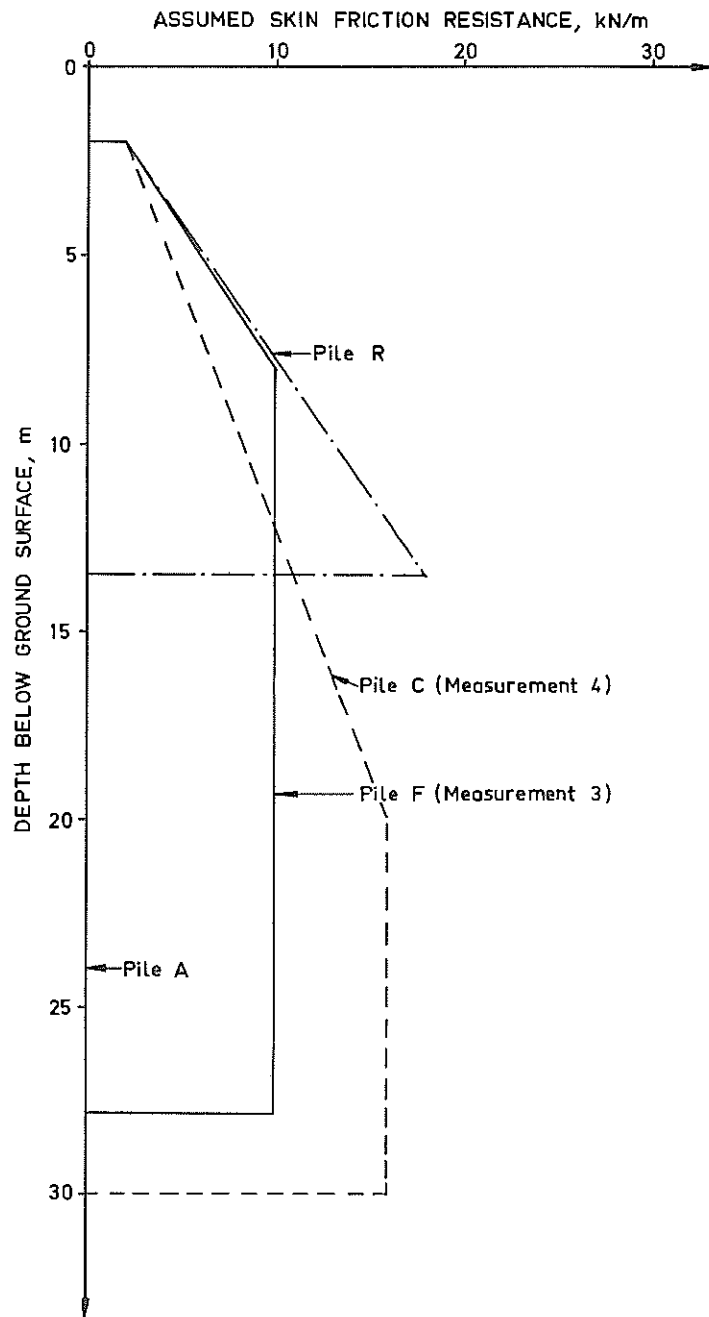


Fig. 33. Assumed distribution of skin friction resistance used for the computer calculation of the stress waves in fig. 34 - 37.

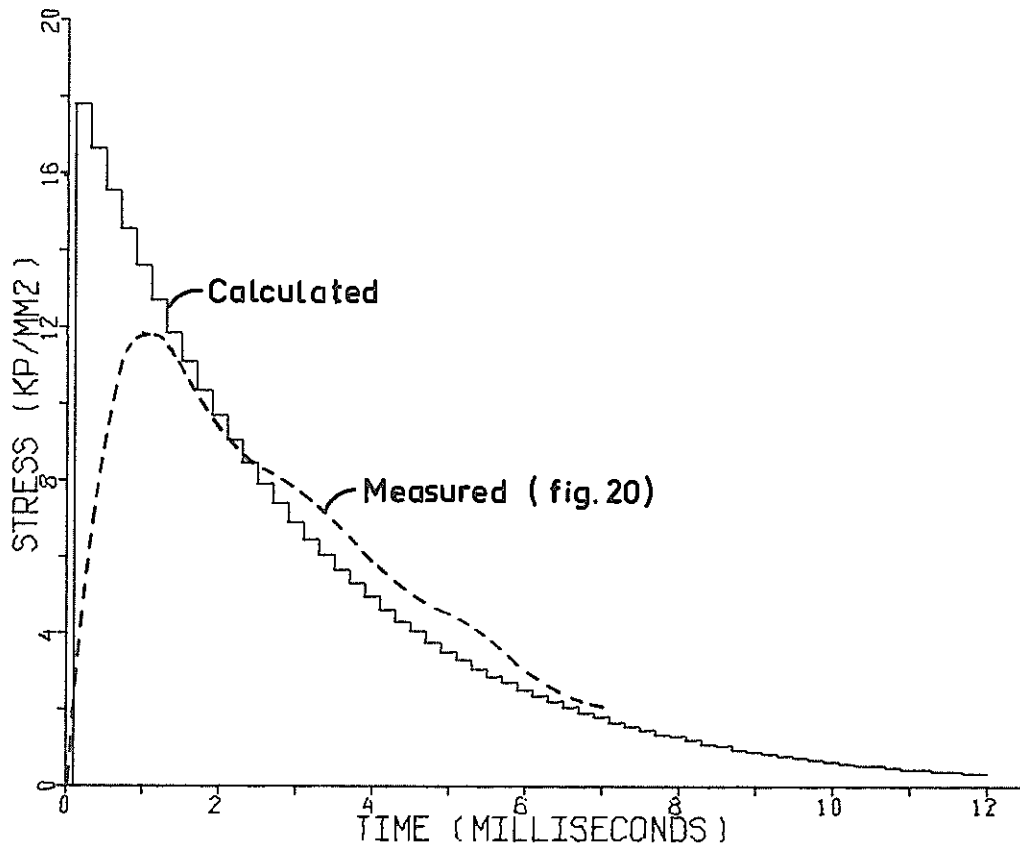


Fig. 34. Comparison between measured and calculated stress waves in Pile A.

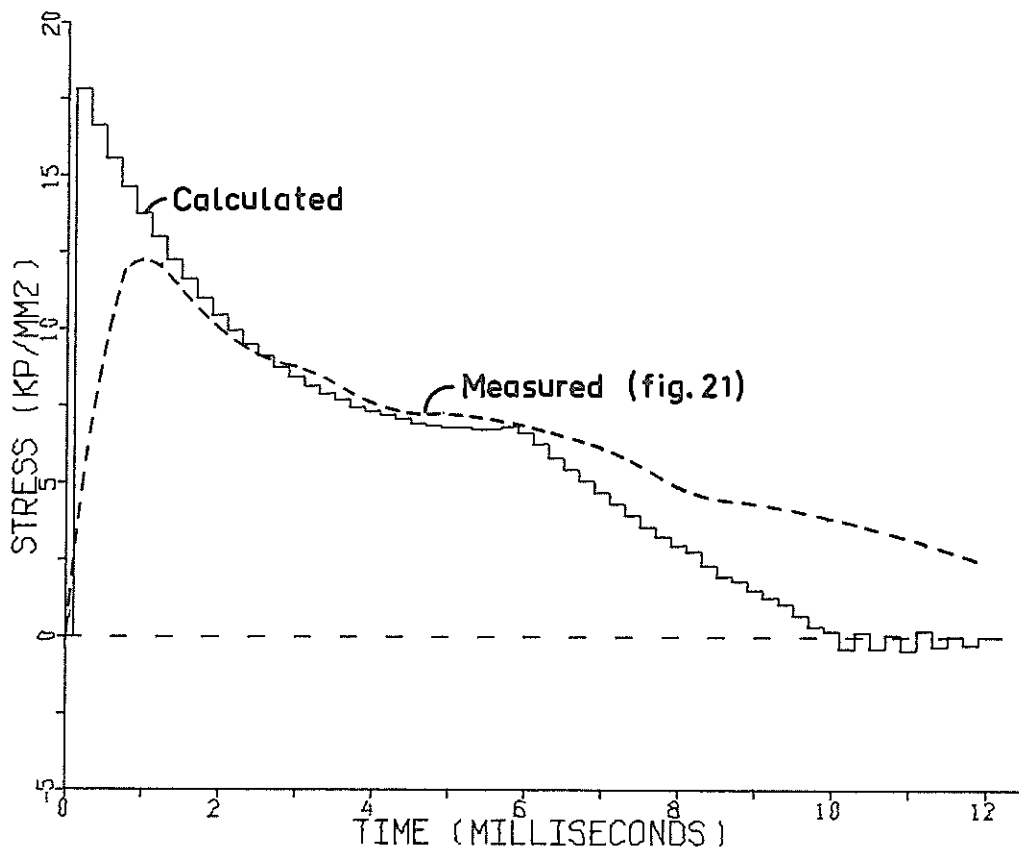


Fig. 35. Comparison between measured and calculated stress waves in Pile C.



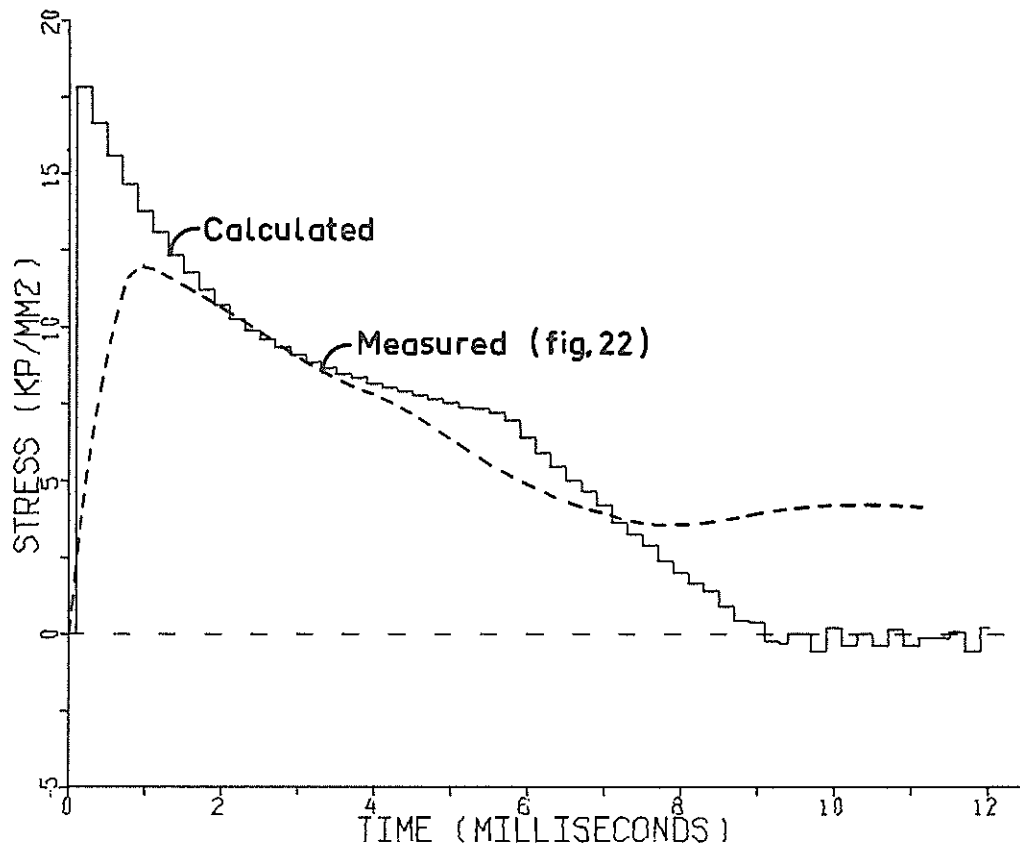


Fig. 36. Comparison between measured and calculated stress waves in Pile F.

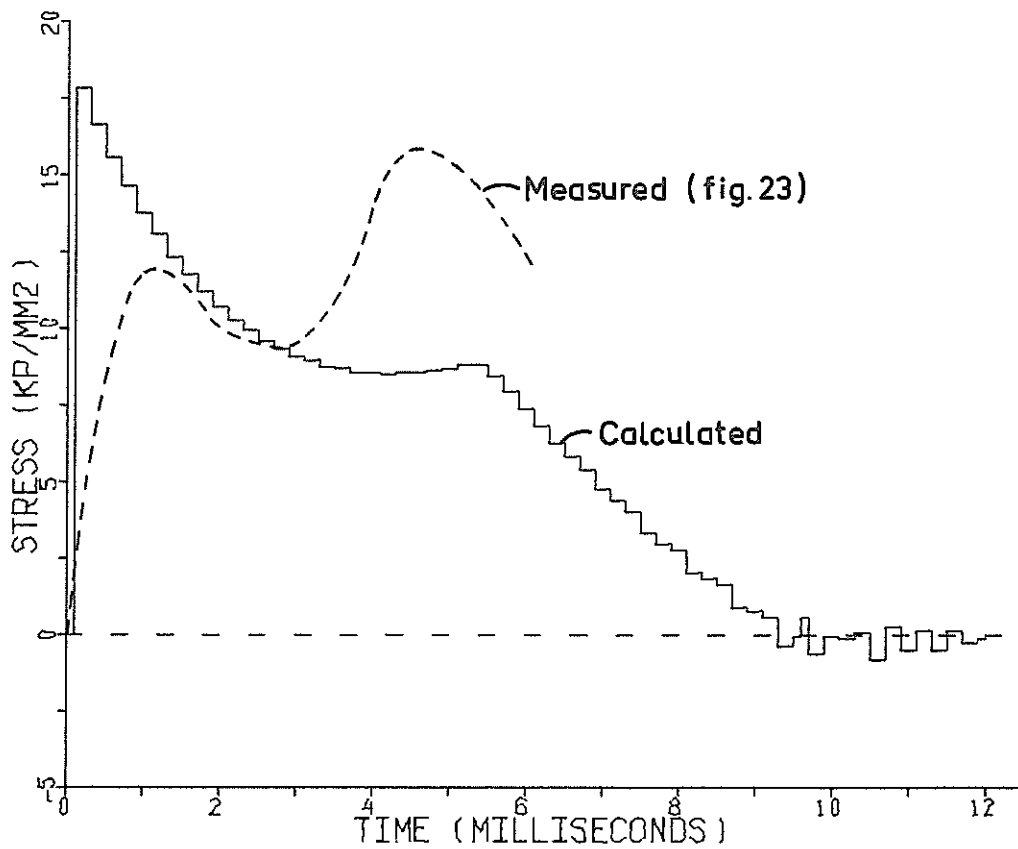


Fig. 37. Comparison between measured and calculated stress waves in Pile R.

The agreement between measured and calculated waves is satisfactory for Piles C and F. The assumed friction resistance along the pile surface is 10 kN/m (670 lb/ft). This corresponds to a damping coefficient of 12 kNs/m<sup>3</sup> (113 lb sec/ft<sup>3</sup>) which is about six times higher than the measured amplitude damping. For Pile R is the agreement between measured and calculated waves not satisfactory even with a very high assumed friction force.

It should, however, be noted that the computer program has been developed for heavy concrete piles and the program has worked well for this particular case. The program does apparently not work equally well for light steel piles.



Fig. 38. Arrangement for pulling tests.

Pulling tests. The two test piles (F and R) which had been driven in sand at Fittja were pulled a few weeks after the driving. The extractor is shown in Fig. 38, and a 30 ton jack operated by a hand pump were used. The resulting force-displacement relationships from the two pulling tests are shown in Fig. 39. The maximum pull-out resistance for the 28 meter long pile F, with a smooth surface, was 85 kN (8.5 metric tons) which corresponds to an average unit

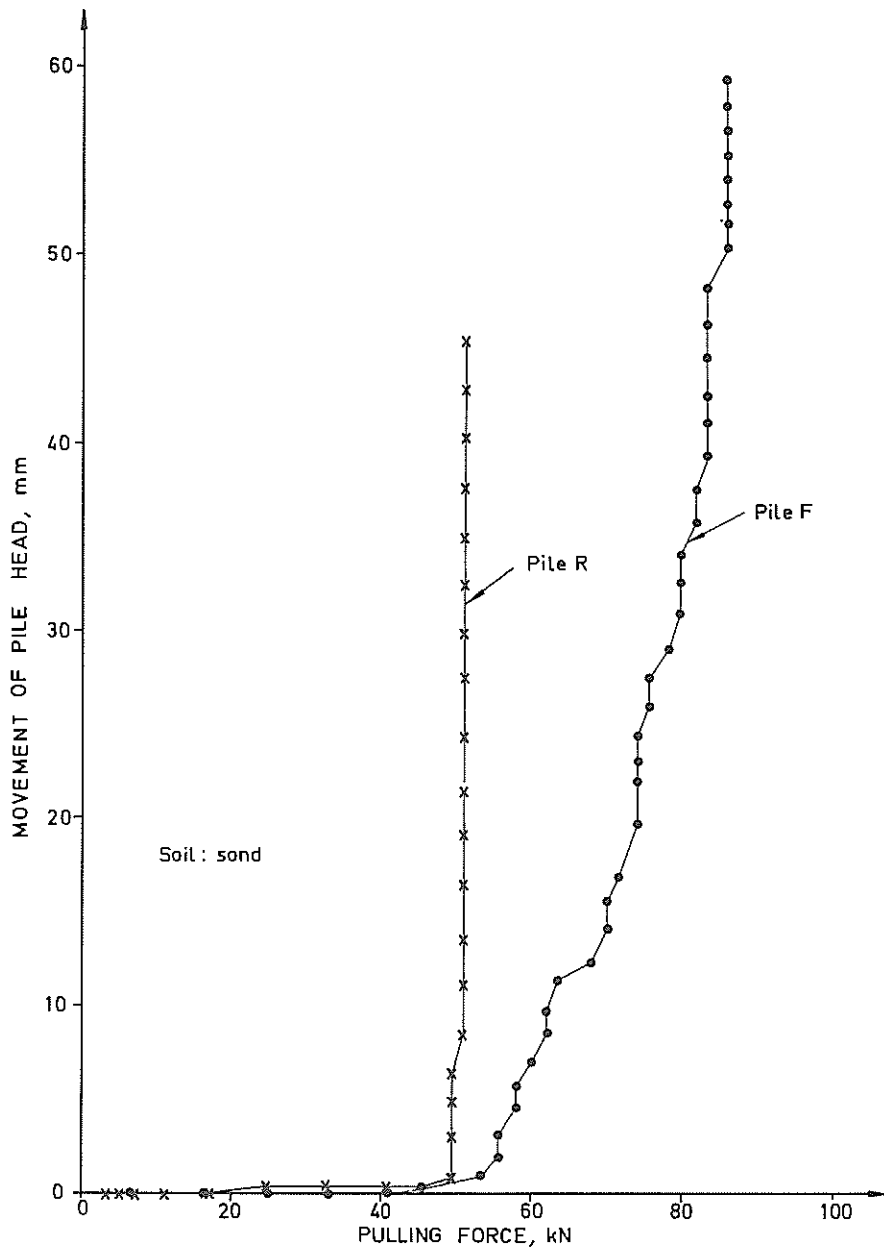


Fig. 39. Load-deformation relationship during pull out tests for Piles F and R.

resistance of  $10.8 \text{ kN/m}^2$  (1.53 psi). The pull-out resistance of the 13.5 meter long Pile R, which had a rough surface, was 51 kN (5.1 metric tons), corresponding to an average unit resistance of  $13.5 \text{ kN/m}^2$  (1.92 psi). Both the total pull-out resistance and the difference in pull-out resistance between the two piles were small.

## 7. CONCLUSIONS

An equation has been developed for the calculation of the damping as the stress wave travels down a pile during the driving. It has been assumed in the derivation of this equation that the damping coefficient  $C_d$  is proportional to the particle velocity of the pile material as indicated by the test results. The test data indicate furthermore that

1. The damping in the steel material and in the welded joints was negligible.
2. The coefficient  $C_d$  was approximately  $3 \text{ kNs/m}^3$  ( $20 \text{ lb sec/ft}^3$ ) for the steel pile in soft clay with a shear strength of 20 to 30  $\text{kN/m}^2$  (2.8 to 4.2 psi) and a sensitivity of about 10.
3. The coefficient  $C_d$  was approximately the same for sand as for soft clay ( $C_d \approx 2 \text{ kNs/m}^3$ ).
4. The coefficient  $C_d$  increased with depth for the investigated clay probably due to the increase of the shear strength with depth. For the tests in sand the coefficient  $C_d$  decreased slightly with depth in contrast to the penetration resistance which increased with depth.
5. The damping coefficient increased 2 to 3 times (to  $4 - 6 \text{ kNs/m}^3$ ) for the pile which had been driven through clay, when the pile was redriven 50 days after the initial driving.
6. The damping coefficient was 2 to 3 times higher ( $4 - 6 \text{ kNs/m}^3$ ) for the pile with rough surface than for the pile with a smooth surface.

The shape and intensity of the stress wave has been back calculated by a method proposed by Vilander (1969), assuming different distributions of the friction force along the pile surface. It was not possible to obtain a satisfactory agreement between calculated and measured values with this method.

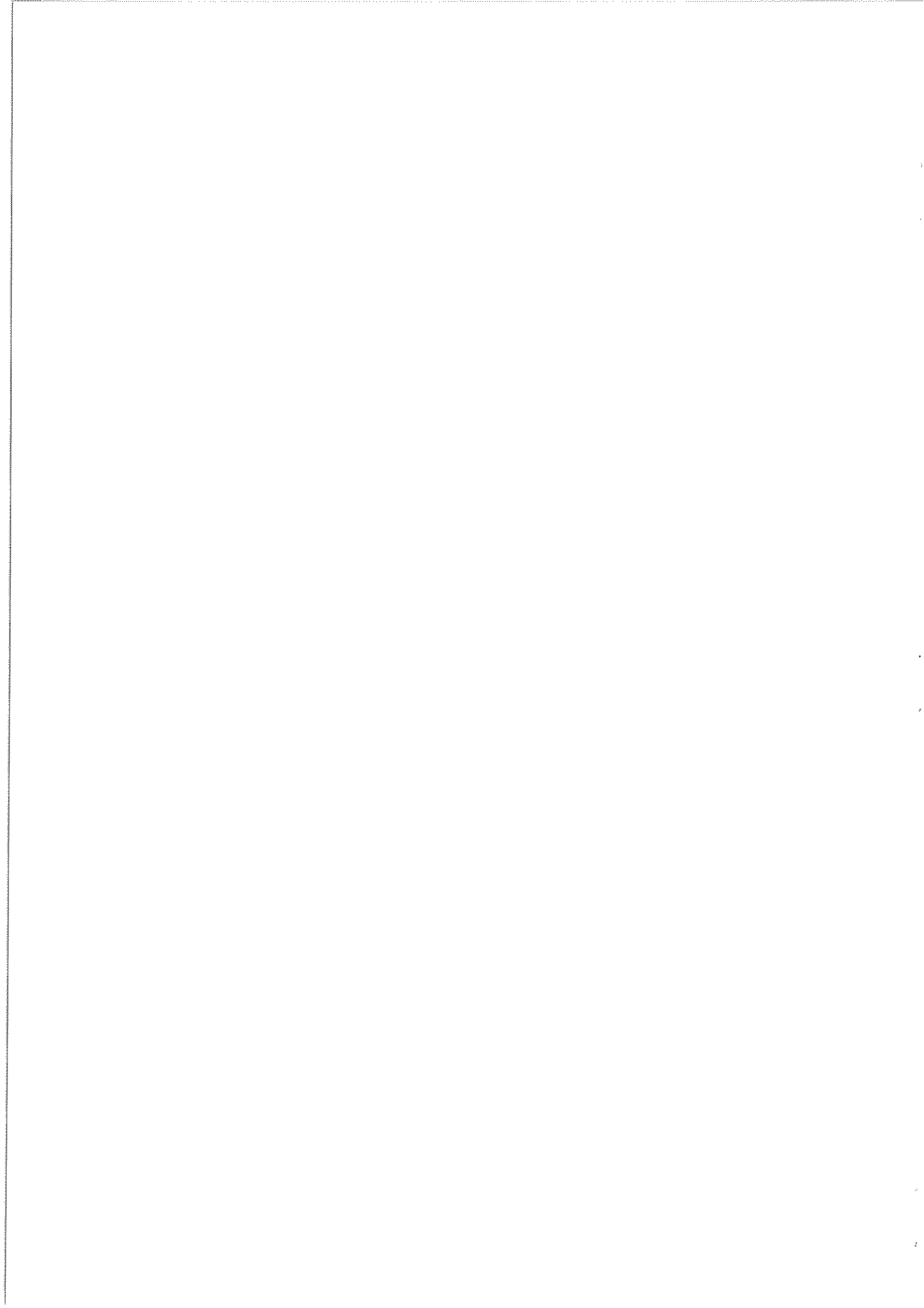
## ACKNOWLEDGEMENTS

This investigation has been supported financially by the Swedish Board for Building Research and by the Swedish Commission for Pile Research. The investigation has been supervised by B. Broms of the Swedish Geotechnical Institute. S.-E. Höök designed the pile driving rig under the direction of U. Bergdahl. The field measurements, which were supervised by G. Fjelkner, were carried out by K. Allard. The computer calculations were made by L. Vilander.

## REFERENCES

- BROMS, B.B. & SILBERMANN, J.O., 1964. Skin friction resistance for piles in cohesionless soils. *Sols-Soils*, Vol. 3, No. 10, p. 33-43.
- BROMS, B.B., 1965. Beräkning av vertikala pålars bärförmåga. R. Swed. Acad. Engng. Sci. Comm. Pile Res., Medd. No. 7. Stockholm. 26 p.
- FISCHER, H-C., 1960. On longitudinal impact. Diss. R. Inst. Technol. Stockholm.
- FJELKNER, G., 1971. Stålpålars bärförmåga. Resultat av fältförsök med lätta slagdon. R. Swed. Acad. Engng. Sci. Comm. Pile Res., Medd. No. 16. Stockholm. 88 p. + 63 p.
- GIBSON, G. & COYLE, H.M., 1968. Soil damping constants related to common soil properties in sands and clays. Texas Transp. Inst. Res. Rep. No. 125-1. Texas. 28 p.
- GLANVILLE, W.H., GRIME, G., FOX, E.N. & DAVIES, W.W., 1938. An investigation of the stresses in reinforced concrete piles during driving. Dep. Scient. a. Indust. Res. Build. Res. Techn. Paper No. 20. London. 111 p.
- KALLSTENIUS, T., 1963. Studies on clay samples taken with standard piston sampler. Swed. Geot. Inst. Proc. No. 21. Stockholm. 210 p.

- ORRJE, O., 1968. Dynamic loading tests on cohesionless soils with free falling weights, compared with static plate loading tests. R. Inst. Technol. Div. Soil Mech. Stockholm. 42 p. + 46 p.
- SMITH, E.A.L., 1960. Pile driving analysis by the wave equation. J. Soil Mech. a. Found. Div. Proc. ASCE, Vol. 86, No. SM4, p. 35-61.
- SOVINC, I., 1969. Driving stresses in open-end steel pipe piles. Acta Technica Academia Scientiarum Hungaricae, Tomus 64 (1-2), p. 217-223. Budapest.
- BFR, 1964. Slagning och provbelastning av långa betongpålar. Försök vid Gubbero i Göteborg, 1964. Statens Råd för Byggnadsforskning, Rapp. No. 99. Stockholm. 230 p.
- SUNDSTRÖM, K-E., 1970. Mätning av fallhejares anslagshastighet vid påslagning. R. Swed. Acad. Engng. Sci. Comm. Pile Res., Särtr. o. Prel. Rapp. No. 28, Stockholm. 13 p.
- VILANDER, L., 1969. Datorberäkning av stötvågsförlopp i pålar medelst variation av modellparametrar. Delrapport 3. R. Swed. Acad. Engng. Sci. Comm. Pile Res., Särtr. o. Prel. Rapp. No. 19, Stockholm. 39 p.







No.		1967	Pris kr. (Sw. crs.)
17.	Om påslagning och påbärighet.	1967	5:—
	1. Dragsprickor i armerade betongpålar. <i>S. Sahlin</i>		
	2. Sprickbildning och utmattning vid slagning av armerade modellpålar av betong. <i>B-G. Hellers</i>		
	3. Bärighet hos släntberg vid statisk belastning av bergspets. Resultat av modellförsök. <i>S-E. Rehnman</i>		
	4. Negativ mantelfriktion. <i>B. H. Fellenius</i>		
	5. Grundläggning på korta pålar. Redogörelse för en försöksserie på NABO-pålar. <i>G. Fjellkner</i>		
	6. Krokiga pålars bärförmåga. <i>B. Broms</i>		
18.	Pålgruppers bärförmåga. <i>B. Broms</i>	1967	10:—
19.	Om stoppslagning av stödpålar. <i>L. Hellman</i>	1967	5:—
20.	Contributions to the First Congress of the International Society of Rock Mechanics, Lisbon 1966.	1967	5:—
	1. A Note on Strength Properties of Rock. <i>B. Broms</i>		
	2. Tensile Strength of Rock Materials. <i>B. Broms</i>		
21.	Recent Quick-Clay Studies.	1967	10:—
	1. Recent Quick-Clay Studies, an Introduction. <i>R. Pusch</i>		
	2. Chemical Aspects of Quick-Clay Formation. <i>R. Söderblom</i>		
	3. Quick-Clay Microstructure. <i>R. Pusch</i>		
22.	Jordtryck vid friktionsmaterial.	1967	30:—
	1. Resultat från mätning av jordtryck mot brolandfäste. <i>B. Broms &amp; I. Ingelson</i>		
	2. Jordtryck mot oeftergivliga konstruktioner. <i>B. Broms</i>		
	3. Metod för beräkning av sambandet mellan jordtryck och deformation hos främst stödmurar och förankringsplattor i friktionsmaterial. <i>B. Broms</i>		
	4. Beräkning av stolpfundament. <i>B. Broms</i>		
23.	Contributions to the Geotechnical Conference on Shear Strength Properties of Natural Soils and Rocks, Oslo 1967.	1968	10:—
	1. Effective Angle of Friction for a Normally Consolidated Clay. <i>R. Brink</i>		
	2. Shear Strength Parameters and Microstructure Characteristics of a Quick Clay of Extremely High Water Content. <i>R. Karlsson &amp; R. Pusch</i>		
	3. Ratio $c/p'$ in Relation to Liquid Limit and Plasticity Index, with Special Reference to Swedish Clays. <i>R. Karlsson &amp; L. Viberg</i>		
24.	A Technique for Investigation of Clay Microstructure. <i>R. Pusch</i>	1968	22:—
25.	A New Settlement Gauge, Pile Driving Effects and Pile Resistance Measurements.	1968	10:—
	1. New Method of Measuring in-situ Settlements. <i>U. Bergdahl &amp; B. Broms</i>		
	2. Effects of Pile Driving on Soil Properties. <i>O. Orrje &amp; B. Broms</i>		
	3. End Bearing and Skin Friction Resistance of Piles. <i>B. Broms &amp; L. Hellman</i>		
26.	Sättningar vid vägbyggnad.	1968	20:—
	Föredrag vid Nordiska Vägtekniska Förbundets konferens i Voksenåsen, Oslo 25—26 mars 1968.		
	1. Geotekniska undersökningar vid bedömning av sättningar. <i>B. Broms</i>		
	2. Teknisk-ekonomisk översikt över anläggningsmetoder för reducering av sättningar i vägar. <i>A. Ekström</i>		
	3. Sättning av verkstadsbyggnad i Stenungsund uppförd på normalkonsoliderad lera. <i>B. Broms &amp; O. Orrje</i>		
27.	Bärförmåga hos släntberg vid statisk belastning av bergspets. Resultat från modellförsök. <i>S-E. Rehnman</i>	1968	15:—

No.			Pris kr. (Sw. crs.)
28.	Bidrag till Nordiska Geoteknikermötet i Göteborg den 5-7 september 1968.	1968	15: -
	1. Nordiskt geotekniskt samarbete och nordiska geoteknikermöten. <i>N. Flodin</i>		
	2. Några resultat av belastningsförsök på lerterräng speciellt med avseende på sekundär konsolidering. <i>G. Lindskog</i>		
	3. Sättningar vid grundläggning med plattor på moränlera i Lund. <i>S. Hansbo, H. Bennermark &amp; U. Kihlblom</i>		
	4. Stabilitetsförbättrande spontkonstruktion för bankfyllningar. <i>O. Wager</i>		
	5. Grundvattenproblem i Stockholms city. <i>G. Lindskog &amp; U. Bergdahl</i>		
	6. Aktuell svensk geoteknisk forskning. <i>B. Broms</i>		
29.	Classification of Soils with Reference to Compaction. <i>B. Broms &amp; L. Forssblad</i>	1968	5: -
30.	Flygbildstolkning som hjälpmedel vid översiktliga grundundersökningar.	1969	10: -
	1. Flygbildstolkning för jordartsbestämning vid samhällsplanering 1-2. <i>U. Kihlblom, L. Viberg &amp; A. Heiner</i>		
	2. Identifiering av berg och bedömning av jorddjup med hjälp av flygbilder. <i>U. Kihlblom</i>		
31.	Nordiskt sonderingsmöte i Stockholm den 5-6 oktober 1967. Föredrag och diskussioner.	1969	30: -
32.	Contributions to the 3rd Budapest Conference on Soil Mechanics and Foundation Engineering, Budapest 1968.	1969	10: -
	1. Swedish Tie-Back Systems for Sheet Pile Walls. <i>B. Broms</i>		
	2. Stability of Cohesive Soils behind Vertical Openings in Sheet Pile Walls. Analysis of a Recent Failure. <i>B. Broms &amp; H. Bennermark</i>		
33.	Seismikdag 1969. Symposium anordnat av Svenska Geotekniska Föreningen den 22 april 1969.	1970	20: -
34.	Något om geotekniken i Sverige samt dess roll i planerings- och byggprocessen. Några debattinlägg och allmänna artiklar.	1970	15: -
	<i>T. Kallstenius</i>		
	1. Geoteknikern i det specialiserade samhället. <i>B. Broms</i>		
	2. Diskussionsinlägg vid konferens om geovetenskaperna, 7 mars 1969.		
	3. Geoteknik i Sverige - utveckling och utvecklingstendenser.		
	4. Geotekniska undersökningar och grundläggningsmetoder.		
	5. Grundläggning på plattor - en allmän översikt.		
35.	Piles - a New Force Gauge, and Bearing Capacity Calculations.	1970	10: -
	1. New Pile Force Gauge for Accurate Measurements of Pile Behavior during and Following Driving. <i>B. Fellenius &amp; Th. Haagen</i>		
	2. Methods of Calculating the Ultimate Bearing Capacity of Piles. A Summary. <i>B. Broms</i>		
36.	Påslagning. Materialegenskaper hos berg och betong.	1970	10: -
	1. Bergets bärförmåga vid punktbelastning. <i>S.-E. Rehnman</i>		
	2. Deformationsegenskaper hos slagna betongpålar. <i>B. Fellenius &amp; T. Eriksson</i>		
37.	Jordtryck mot grundmurar.	1970	10: -
	1. Jordtryck mot grundmurar av Lecablock. <i>S.-E. Rehnman &amp; B. Broms</i>		
	2. Beräkning av jordtryck mot källarväggar. <i>B. Broms</i>		
38.	Provtagningsdag 1969. Symposium anordnat av Svenska Geotekniska Föreningen den 28 oktober 1969.	1970	25: -

No.		1970	Pris kr. (Sw. crs.)
39.	Morändag 1969. Symposium anordnat av Svenska Geotekniska Föreningen den 3 december 1969.	1970	25:—
40.	Stability and Strengthening of Rock Tunnels in Scandinavia. 1. Correlation of Seismic Refraction Velocities and Rock Support Requirements in Swedish Tunnels. <i>O. S. Cecil</i> 2. Problems with Swelling Clays in Norwegian Underground Constructions in Hard-Rocks. <i>R. Selmer-Olsen</i>	1971	25:—
41.	Stålpåars bärförmåga. Resultat av fältförsök med lätta slagdon. <i>G. Fjellkner</i>	1971	30:—
42.	Contributions to the Seventh International Conference on Soil Mechanics and Foundation Engineering, Mexico 1969.	1971	15:—
43.	Centrically Loaded Infinite Strip on a Single-Layer Elastic Foundation — Solution in Closed Form According to the Boussinesq Theory. <i>B-G. Hellers &amp; O. Orrje</i>	1972	20:—
44.	On the Bearing Capacity of Driven Piles. 1. Methods Used in Sweden to Evaluate the Bearing Capacity of End-Bearing Precast Concrete Piles. <i>B. Broms &amp; L. Hellman</i> 2. Discussions at the Conference, Behaviour of Piles, London 1970. <i>B. Fellenius, B. Broms &amp; G. Fjellkner</i> 3. Bearing Capacity of Piles Driven into Rock. With Discussion. <i>S-E. Rehnman &amp; B. Broms</i> 4. Bearing Capacity of Cyclically Loaded Piles. <i>B. Broms</i> 5. Bearing Capacity of End-Bearing Piles Driven to Rock. <i>S-E. Rehnman &amp; B. Broms</i>	1972	20:—
45.	Quality in Soil Sampling. 1. Secondary Mechanical Disturbance. Effects in Cohesive Soil Samples. <i>T. Kallstenius</i> 2. Sampling of Sand and Moraine with the Swedish Foil Sampler. <i>B. Broms &amp; A. Hallén</i>	1972	10:—
46.	Geoteknisk flygbildstolkning. En undersökning av metodens tillförlitlighet. <i>L. Viberg</i>	1972	1) <sup>1)</sup>
47.	Some Experiments on Hollow Cylinder Clay Specimens. <i>A. K. Jamal</i>	1972	10:—
48.	Geobildtolkning vid vägprojektering. Rapport från försöksverksamhet 1969—71. <i>U. Kihlblom, L. Viberg, A. Heiner &amp; K. Hellman-Lutti</i>	1972	20:—
49.	Lerzoner i berganläggningar. Diskussionsmöte anordnat av IVA den 7 oktober 1970.	1972	30:—
50.	Damping of Stress Waves in Piles during Driving. Results from Field Tests. <i>G. Fjellkner &amp; B. Broms</i>	1972	30:—

<sup>1)</sup> Distribution: AB Svensk Byggtjänst